



Network arch bridge

Optimization of the arch applying simple loads



SEVERIN LIE RUDI

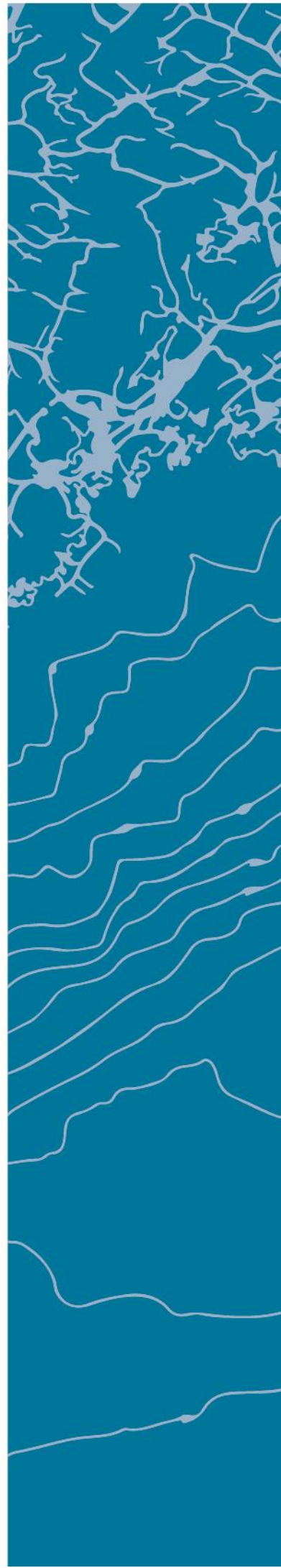
SUPERVISOR

Songxiong Ding

University of Agder, 2019

Faculty of Engineering and Science

Institute of Civil and Constructional Engineering



Declaration

1.	With this statement I declare that this master thesis is my own work and that I have not used other sources or received other help than what is marked as such.	<input checked="" type="checkbox"/>
2.	Furthermore, with this statement I declare that this master thesis: <ul style="list-style-type: none"> - was not previously submitted to another academic institution in Norway or any other country. - does not refer to external sources without this being properly marked. - does not refer to own earlier work without this being properly marked. - includes a bibliography with all sources. - is no copy or duplicate of other's work. 	<input checked="" type="checkbox"/>
3.	I am aware that a violation of the statements above can cause nullification of the examination and exclusion from universities in Norway, cf. Universitets- og høyskoleloven §§4-7 and 4-8 and Forskrift om eksamen §§ 31.	<input checked="" type="checkbox"/>
4.	I am aware that all submitted works can be checked for plagiarism.	<input checked="" type="checkbox"/>
5.	I am aware that the University of Agder will treat all cases with suspicion for cheating according to the university's guidelines as cheating.	<input checked="" type="checkbox"/>
6.	I have studied the rules and guidelines concerning the use of sources and references on the library's webpages.	<input checked="" type="checkbox"/>

Publishing Agreement

Authorization for Electronic Publishing of the Master Thesis

The author has the copyright for the work. This includes amongst other things the exclusive right to make the work available for the public (Åndsverkloven. §2).

All works that fulfil the requirements will be registered and published in Brage Aura and on UiA's webpages with the author's approval.

Works that are excluded from the public or subject to professional secrecy or confidentiality will not be published.

I hereby give the University of Agder the gratuitous right to make this master thesis available for electronic publishing:

JA NEI

Is this master thesis confidential?

JA NEI

- If yes:

Can the work be published once the obligation for confidentiality has ended?

JA NEI

Is this master thesis excluded from the public?

JA NEI

Preface

This thesis is the final part of the master study in civil and constructional engineering, class of 2017 at University of Agder (UiA). The master thesis has an extent of 30 ECTS.

This task was very interesting for me as the research on the area is quite limited and gives room for development. During my bachelor and master study there has not been a lot of focus on bridge construction. For a structural engineer living in Norway knowledge about bridges can be useful in work situations. After working with network arch bridges for the past semester I have got a deeper understanding of designing bridge structures and I am curious about future projects.

The project was carried out as an individual study and in collaboration with UiA.

I would like to thank my supervisor, Songxing Ding for guiding me through the thesis and giving me constructive feedback on my work along the way.

Abstract

This master thesis gives insight in structural behavior of network arch bridges. When designed with circular arches the bending moments tend to rise near the bridge ends. As suggestions for improving this problem two alternative arch geometries are investigated; arch with elliptical shape and a three-center arch shape.

The arch geometries are modelled with different radius ratios. In addition, different variables are changed on the models which includes; arch rise, hanger inclination, number of hangers and the transition point between the curvatures. Two-dimensional numerical calculations are done using structural software. Only simple loads are applied to the bridges as the task is based on comparing the different arches.

After analyzing the results, it is evident that a reduced radius ratio for both elliptical arches and three-center arches improves the bending moments near the arch ends.

Table of contents

Publishing Agreement	1
Preface.....	2
Abstract	3
Table of contents.....	4
Figure list	6
Table list	8
1 Introduction.....	1
1.1 Goal	1
1.2 Background.....	1
1.3 Delimitations	2
2 Significance of the work	3
3 Literature study	4
3.1 Historical overview	4
3.2 What is a network arch bridge?	6
3.3 The arch.....	7
3.3.1 Geometry of the arch	8
3.4 The hangers	12
3.4.1 Hanger types.....	12
3.4.2 Hanger arrangement	13
3.5 Main girder and deck.....	14
3.6 Analysis.....	15
3.6.1 Solver setup	15
3.7 Buckling	17
3.8 Moving loads	19
3.8.1 Envelopes	19
3.9 Construction of network arches.....	19
4 Research question	20
4.1 Sub questions	20
5 Method.....	21
5.1 The arch geometries.....	21
5.1.1 Circular arch.....	21
5.1.2 Elliptical	22
5.1.3 Three-center arch (TCA)	23
5.2 Geometries	25

5.2.1	Explanation of variations	26
5.3	Modeling.....	27
5.3.1	AutoCAD	27
5.3.2	Robot Structural Analysis (RSA).....	27
5.4	Weakness with the method	31
6	Results	32
6.1	Bending moments TCA	32
6.1.1	Positive bending moments.....	32
6.1.2	Negative bending moments	34
6.2	Axial forces TCA	36
6.3	Bending moments ellipse	38
6.3.1	Positive bending moments.....	38
6.3.2	Negative bending moments	40
6.4	Axial forces ellipse	42
6.5	Relaxation of hangers.....	44
6.6	Comparison	45
6.6.1	In-plane buckling modes	45
6.6.2	Moving loads	46
6.6.3	Forces	46
7	Discussion	47
7.1	Circular arch.....	47
7.2	TCA.....	47
7.3	Elliptical arch	48
7.4	Comparison	49
8	Conclusion	50
9	Suggestions for further work.....	51
10	References.....	52
11	Table of appendix.....	53

Figure list

Figure 1.1: Rise of bending moments at the arch ends [own figure].....	1
Figure 3.1: Three Center Arch in Amsterdam. [3]	4
Figure 3.2: Da Vinci's drawing, right: Lenticular girder in Shanghai [4].	5
Figure 3.3: Half span load, top: deformation, bottom: bending moments [own figure].....	6
Figure 3.4: Brandangersundbrua with circular hollow arches [9].....	7
Figure 3.5: Tsukani Bridge with box-section arches [10].	7
Figure 3.6: Happy hollow zoo with wide flange arches [11].	7
Figure 3.7: UDL over a parabolic arch [12].....	8
Figure 3.8: Moment in arch as a consequence of eccentricity [own figure].....	9
Figure 3.9: Parabolic arch subjected to vertical UDL [12].	9
Figure 3.10: Stress utilization for the different arch shapes [13].....	10
Figure 3.11: Left: Welded connection for steel rod, right: fork connection for spiral strand cable [16].	12
Figure 3.12: Radial hanger arrangement [15].	13
Figure 3.13: Crossing angles for different bridge spans, relevant to radial hanger arrangement [13].	14
Figure 3.14: Left: concentrated load on a deck with low stiffness, right: concentrated load on bridge with high stiffness	14
Figure 3.15: Incremental method of non-linear analysis [17].....	15
Figure 3.16: In-plane buckling of network arch bridge showing the buckling mode shape [6].	17
Figure 5.1: Circular arch shape [own figure].	21
Figure 5.2: Elliptical arch shape [own figure].	22
Figure 5.3: Relation between r_a and r_b , outlined region represents the used range for the bridge [own figure].	22
Figure 5.4: Three center arch where span length, w is constant [own figure].	23
Figure 5.5: Three center arch where height, h is constant [own figure].....	23
Figure 5.6: Sketch used to obtain the expression for W [own figure].	24
Figure 5.7: Number of elements used in numerical calculations [own figure].	27
Figure 5.8: Applied loads [own figure].	29
Figure 5.9: Adjustment of hangers at bridge end. Left: before, right: after [own figure].....	30
Figure 6.1: Full load.	32
Figure 6.2: Half load.	33
Figure 6.3: Full load.	34
Figure 6.4: Half load.	35
Figure 6.5: Full load.	36
Figure 6.6: Half load.	37

Figure 6.7: Full load.	38
Figure 6.8: Half load.	39
Figure 6.9: Full load.	40
Figure 6.10: Half load.	41
Figure 6.11: Full load.	42
Figure 6.12: Half load.	43
Figure 6.13: Moment envelope for model A.	46
Figure 6.14: Moment envelope for model C.	46
Figure 6.15: Moment envelope for model B.	46

Table list

Table 6.1: Equations.	24
Table 6.2: Models for TCA.	25
Table 6.3: Models for elliptical arch.	25
Table 6.4: Material types.	27
Table 6.5: Load combinations.	29
Table 7.2: Number of relaxed hangers for det different models.	44
Table 7.3: Buckling mode shape and critical coefficients for the optimal geometries [RSA].	45
Table 7.4: Comparison of results for the different arch shapes.	46

1 Introduction

1.1 Goal

The goal of this thesis is to contribute to the future development of network arch bridges. Optimization of structures in general lead to reductions in material use, costs and most importantly carbon emissions.

My main objective of this thesis is to get a deeper understanding of what goes into the design of a bridge by doing literature study. The goal is also to get more knowledge of doing numerical calculations in structural software as this is valuable when I am going to start my engineering career.

1.2 Background

The construction industry is growing in parallel with the growth of the population. Focus on finding solutions that are innovative, cost effective and sustainable is getting more and more important. The network arch bridge is a structure for the future. Its slender, light, aesthetic, most parts can be prefabricated, it can be transported to construction sites by road or river. As Norway is a country with valleys and fjords, the network arch bridges versatility fits perfect.

The first network arch bridge, Håkkadalsbrua was erected in 1963. For the first decade the number of bridges constructed was low. Today we can see that the network arch bridge is growing in popularity all over the world.

After meetings with Per Tveit and Songxiong Ding autumn 2018 we discussed the possibility of writing a thesis about the curvature of the network arch bridge. For circular arches the bending moments tend to rise near the bridge end, see figure 1.1. The thesis focuses on optimization of the arch curvature in network arch bridges.

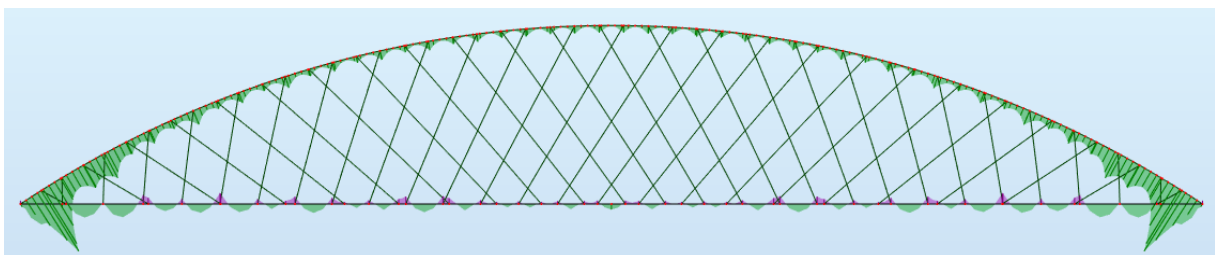


Figure 1.1: Rise of bending moments at the arch ends [own figure].

1.3 Delimitations

Limited time and resources make it important to set boundaries for the thesis. The focus has been to investigate the arch geometry, and not the design of network arch bridges. As this thesis is based on the experimental method where results are highly dependent on a lot of numerical calculations of different models, the margin of error must be low. Therefore, in agreement with my supervisor, I decided that following simplifications to the calculations was reasonable:

- Loads were simplified into unit loads and load combinations are limited. The reason is that the thesis is based on comparison of different arch geometries where the magnitude of the load is not as important, as long as it is the same for all the different models.
- The bridge models are only analyzed by using two-dimensional calculations in software.

2 Significance of the work

Network arch bridges are slender bridge structures with low weight. A study done by Per Tveit shows that material use is considerably lower than for equivalent bridge structures.

Deck and arches can be prefabricated at a manufacturing plant. Work under controlled environments leads to better *safety, health and environment (SHE)* and calls for more effective construction. The assembly on the construction site mostly consists of welding the arches and hanger connections. This is repetitive work where the risk of accidents is low.

At Sunndalsøra a network arch bridge was constructed in 2016. At first the bridge was placed at a temporary location, before it was moved into its final place. To be able to move a whole bridge to a new location is very valuable. This also leads to the possibility for the bridge to be reused when its replaced by a new bridge. Smaller network arch bridges can be transported along the river which means that they can be erected in places that has limited access by road, which also leads to less impact on the areas around the construction site.

This master thesis emphasizes the reduction of forces in the arch of network arch bridges. If it's possible to reduce these forces that also means that smaller arch cross-sections can be used. Yet again this reduces the steel quantity which is economically and environmentally beneficial. Up till now most of network arch bridges are constructed with circular arches. The reason for this is almost exclusively because of ease of construction. If an arch shape with better structural properties also can be easy to construct it might be competitive with the circular arch. An arch consisting of one curvature at the wind portal and another for the rest of the arch might be just that.

Additionally, the network arch bridge is a very aesthetically pleasing structure which blends into the environment. Further research and development of the bridge structure makes it more competitive and maybe we will see a lot more of these beautiful structures in the future.

3 Literature study

3.1 Historical overview

Back in the 13th century BC the first bridge structures understood by men was constructed. These were stone structures constructed utilizing the arch shape to transfer the loads to the abutments [1].

In the 19th century the first set of “rules” for masonry bridge constructions was formed. These rules were mainly based on the aesthetic aspect of the structure and to establish the structural form for the bridge. The rules were essentially of an empirical nature.

The different shapes of the arch were first limited to a few recurring types: full semi-circular arch, circular or segmental arch. The semi-circular arch was advantageous because the compressive forces in the arch were transferred vertically to the springers.

Anses de panier arches became normal to use in the end of the 18th century. It's an arch compiled of curves with more than one center. The most widespread *anses de panier* is the three-center arch consisting of two smaller radius arches at the abutment area that is blended into one larger radius arch at the crown, see figure 3.1.

During the early 1900s this bridge type was widely criticized for not being aesthetically pleasing because of the large variation of the curvature [2].



Figure 3.1: Three Center Arch in Amsterdam. [3]

Later, the “semi-ellipse” was widely used because of the simplicity in calculating the shape of the curve. For masonry arch bridges this was not an especially good design since compressive forces in the arch were transferred as both vertical and horizontal components in the abutment. The horizontal forces were not easy to restrain.

The first sign of a tied arch bridge, also called *bowstring arches*, *Nielsen bridges*, *Lohse girder* and *network arches* were truss bridges with a curved upper chord/arch. Leonardo Da Vinci draw such a bridge back in 1482. Decades later, in 1796 the American engineer Robert Fulton designed a bridge which he called a “bowstring”. The idea was based on an arch where concentrated loads were uniformly distributed by trusses, and that the horizontal forces from the compression in the arch were taken up by a tie in between the arch ends, instead of the abutment.

Through the 19th century many different types of arch bridges were built. Some examples are the bridges over Erie Canal, in New York, constructed 1850-1870. Around the same time the lenticular girder was developed, a truss with curved top and bottom chord, the traffic lanes would be an addition to the bottom chord, see figure 3.2. This design was not very practical when handling traffic, so around 1860, engineers began using trusses where only the top chord was shaped as an arch, so that the bottom chord could handle traffic directly.



Figure 3.2: Da Vinci's drawing, right: Lenticular girder in Shanghai [4].

The first tied arch bridge with vertical hangers were built by Austrian engineer Josef Langer in 1883. Until this day this bridge design is still in use.

In the 1920's Danish engineer Octavius F. Nielsen came up with the idea of using inclined hangers instead of vertical hangers used in tied-arch bridges. Due to limitations in the analysis, the design had to be simplified so that none of the inclined hangers intersected. This bridge design had a high slenderness, and could reach spans of up to 145 m.

The Nielsen bridge inspired engineer Per Tveit to start further development of these bridges. By using new analysis methods that allowed him to calculate and develop a tied-arch bridge with inclined hangers where some of them cross each other at least twice. He called it the “Network Arch Bridge” [5]. To date, the network arch bridge is the latest development of the tied-arch bridge.

In the early stage of development Tveit suggested to his professor that the arch should be part of an ellipse, but the professor urged him to use arches that were part of a circle instead. It took a long time for Tveit to forget about the idea of using an elliptical arch shape [6].

3.2 What is a network arch bridge?

The network arch bridge can be compared to a simply supported I-beam. The arch acts as the compression flange, the main girders as the tension flange and the inclined hangers takes the shear force working as the web. The hangers distribute the force between the tie and arch so that little bending occur.

The main difference between the network arch bridge and a tied arch bridge with vertical hangers becomes evident when only half of the bridge span is loaded. For the tied arch bridge, the axial forces in the arch and tie decreases, but the arch moves towards the unloaded side, which leads to an increase in both deflection and bending moments. When the network arch bridge is loaded on half the span the inclined hangers contributes to distribute the forces in an angle to the arch, where the cross section has larger stiffness, which leads to a decrease in bending moments and deformation, this is described in figure 3.3.

As the network arch bridge is subjected to small moments in both arch and tie, a reduction of the cross-sections resistance to bending (moment of inertia) can be achieved for the different structural parts. This can lead to a reduction of cross-sections as the resistance against bending is defined from the cross-sectional area. This means that network arch bridges have low self-weight, and material costs gets lower [7, 8].

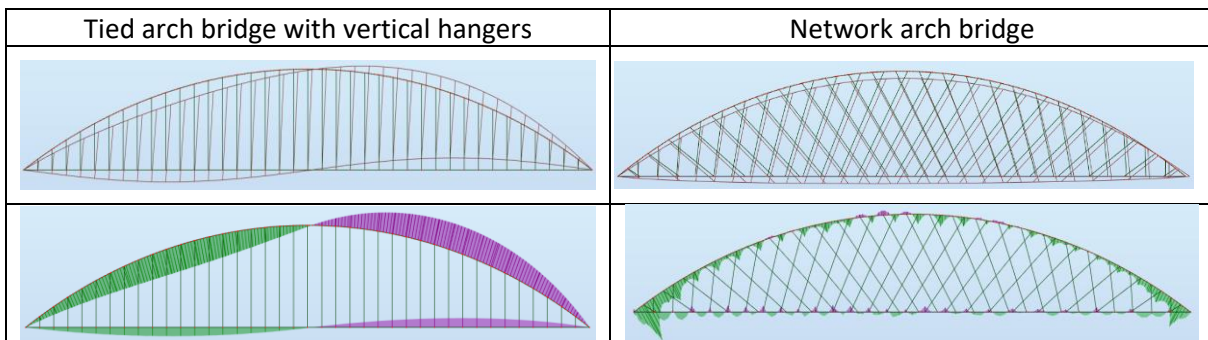


Figure 3.3: Half span load, top: deformation, bottom: bending moments [own figure].

3.3 The arch

Network arch bridges are for the most part built with arches in steel. Prefabrication and ease of transport makes it the most effective and economical material to use.

A variety of cross-sections are used for network arch bridges. American wide flange beams, box-sections and circular hollow sections are some of the types. Instability of the arch is most likely to happen out of the arch plane. For that reason, higher stiffness (EI) is required horizontally.

So, the American wide flanged beams are tilted with their strong axis out of plane. Circular and box sections have large stiffness both vertically and horizontally and are therefore ideal for arches.

For constructional purposes the wide flanged beam is desirable because of the simple connections between hangers and the arch web, it also allows for easy construction of the wind bracing at the arch flanges [8].



Figure 3.4: Brandangersundbrua with circular hollow arches [9].



Figure 3.5: Tsukani Bridge with box-section arches [10].



Figure 3.6: Happy hollow zoo with wide flange arches [11].

3.3.1 Geometry of the arch

The arch of the network arch bridge is most significant for the mechanical properties of the structure. How the arch geometry is obtained are dependent on different parameters:

- The shape of the arch
- Rise of the arch

A pinned beam subjected to a uniformly distributed load (UDL) over the whole span will give a moment diagram that has a parabolic shape. For tied-arch bridges with vertical hangers the shape of the arch is parabolic for exactly this reason. When the UDL is “applied” to the arch, the moment is cancelled out, as the shape of the arch is the same as the moment diagram. An arch with close to no bending moment is preferable [12p. 479].

This works because forces from the permanent loads and live loads over the whole bridge span is distributed through the vertical hangers and into the arch, see figure 3.7.

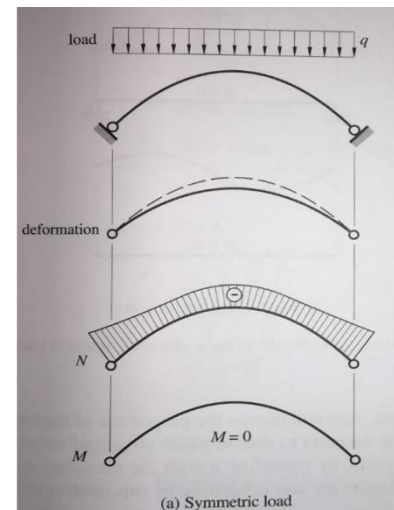


Figure 3.7: UDL over a parabolic arch [12].

The case is different for network arch bridges. Here the loads from the lower chord is distributed through the inclined hangers into the arch. Ideally the force should be perpendicular to the arch neutral axis. In that case, the arch would be loaded radially which correspond to an arch shape that supports radial loading, hence the circular shape [13].

Per Tveit argued in [6] that the shape of the arch should be close to a second-degree parabola if the bridge is built with vertical hangers. For steel arches he recommends that a circular shape is used when designing a network arch bridge. The same argument was made by Pipinato [14] and Teich [13p. 247]

Other advantages with using circular arches in relation to parabolic arch is that it shortens the wind portal of the bridge, gives more even axial force in the middle of the arch, and is easier to construct. Today the circular arch shape is the most widely used arch geometry for network arch bridges [6p. B-12].

Ideally the shape of the arch should coincide with the compression line defined by the forces due to the loads. This will result in only normal forces in the arch. However, because the loads are rarely uniformly distributed, some bending moments arise in the arch. The bending moment at a given point of the arch is defined as the normal force acting at this point times its eccentricity relative to the axis of the arch [12]. In general, this can be described as: $M_x = N_x \times e$, see figure 3.8.

Figure 3.9 shows how a parabolic arch subjected to uniformly distributed vertical load. No bending moments arise for this particular case.

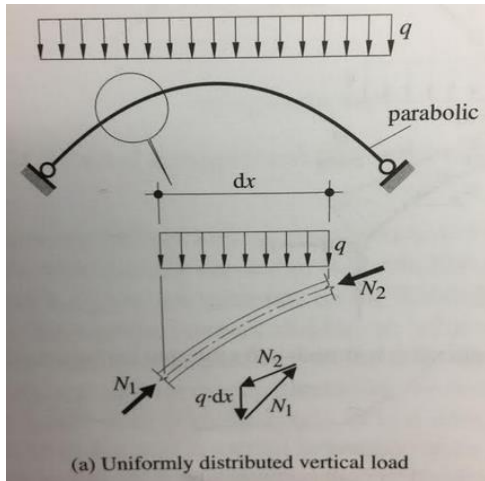


Figure 3.9: Parabolic arch subjected to vertical UDL [12].

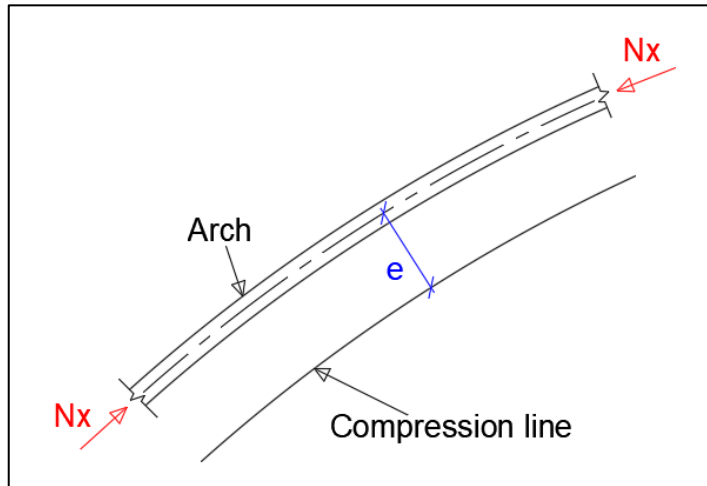


Figure 3.8: Moment in arch as a consequence of eccentricity [own figure]

When analyzing the bending moments in a circular arch, it is clear that the moments increase near the ends of the arch. Bruun and Shanack [15p. 63] explored the possibility of reducing the curvature at ends of the arch. A three-center arch was used in their studies, and the result showed that a reduced ratio at the end of the bridge hardly effected the bending moment or the hanger forces. They saw a reduction in the axial forces because of the steeper angle of the arch at the end. It was concluded that reducing the radius ratio to 0.8 is positive for the wind portal but has no negative effects on hanger forces and bending moments in the arch.

Furthermore, Teich [13p. 234-246] did a more thorough investigation on the effect of changing the arch shape to minimize the bending moments. His research compared circular arches, parabolic arches, elliptical arches and arches with double radius (three-center arch). These are some main points of what his findings were:

- Parabolic arch shape should not be used in the design of network arch bridges. This is because the bending moments increase substantially as the parabolic shape deviates from the compression line of the network arch bridge.
- By investigating the optimal ratio for three center arches and elliptical arches, he concluded with the following: For three center arches the optimal radius ratio was 0.5 and for elliptical arch the optimal ratio was a little bit higher at 0.55.
- As the ratio decreases the shape of the arch converges to a two-hinged frame. As a consequence of this the negative moments (upper side of the arch) at the wind portal rises.

Figure 3.10 illustrates the maximum stress utilization that Teich found for the different arch shapes. The models are analyzed using 3D-simulation with full bridge load.

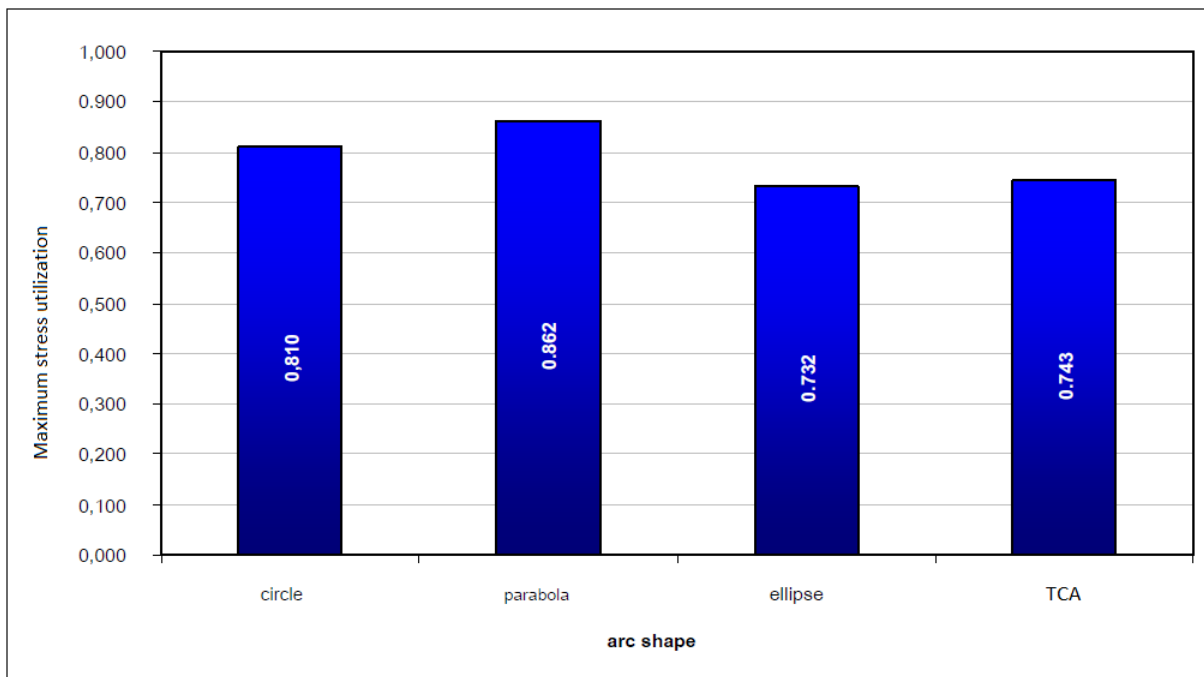


Figure 3.10: Stress utilization for the different arch shapes [13].

Rise of the arch

The height of the arch is for most of the cases related to the aesthetic qualities of the bridge. If the rise of the arch is too high it will not blend into the surroundings [6p. B-1]. Per Tveit said in TNA that; “The arch rise should be about 15 % of the span; larger arch rises decrease internal forces but respecting aesthetics it should not exceed 17 % of the span” [8].

The decrease in axial force can be seen from the following.

If a tied-arch bridge with vertical hangers are considered, this expression for axial force at the top of the arch is given:

$$N_d = \frac{q_d \times W^2}{8 \times H} \quad (3.1)$$

Where:

q_d Uniformly distributed line load over the whole span.
 W Bridge span.
 H Rise of the arch.

For a network arch bridge an additional horizontal component comes from the inclined hangers. The formula was deduced by Tveit, which adds the contribution from the hanger force [8p. 5a].

$$N_d = \frac{q_d \times W^2}{8 \times H} + \frac{H \times q_d}{2 * \tan^2 \alpha} \quad (3.2)$$

Where:

α Angle of the hangers relative to the arch.

If the rise of the arch is increased, it is clear from the formula that the axial force in the middle of the arch span will decrease.

3.4 The hangers

The distribution of forces in the arch are highly dependent on the arrangement of the hangers. This being hanger inclination, number of hangers and the locations of the top and bottom nodes of the hangers with respect to the arch and tie [13].

Under ideal load conditions all hangers contribute to the arch being fully supported in the arch plane. In some load cases (often asymmetrical loading) hangers can become relaxed, these hangers stop supporting the arch which could cause global instability of the whole bridge structure.

3.4.1 Hanger types

- **Steel rod hangers** with circular cross-section. These rods can be connected to the arch and tie by welded hanger connections or bolted connections, often fork connections are used. These types of hangers have good fatigue life and are relatively cheap if the welded type is used, see figure 3.11.
- **Cable hangers** are often connected by anchorages which are fixed to the cables, also for connections are used to mount the cables to the chords. Three types of cables are used: spiral strand, locked coil or parallel strand, see figure 3.11 [16].



Figure 3.11: Left: Welded connection for steel rod, right: fork connection for spiral strand cable [16].

Rods are often used because they have several benefits compared to cables:

- Joints are simple
- Rods are easily prestressed without the need of special equipment
- Their modulus of elasticity is approximately 15 % higher than cables

For arch bridges with a high rise, which leads to long hangers, cables are advantageous. This is because the length of the rods when manufactured are limited. Rods can be welded to increase length. However, this must be carefully carried out, due to the risk of fatigue or brittle fracture [12].

3.4.2 Hanger arrangement

As mentioned earlier the arrangement of the hangers is of great importance to the static system of a network arch bridge. Unfortunately, the bridges being built have hanger arrangements that are based on the ease of construction and aesthetics. Teich [13] developed a guideline on how to optimize the hanger arrangement. The optimal hanger arrangement is obtained by following these structural parameters:

- Minimizing the bending moments in the arch and tie
- Sufficient resistance against hanger relaxation
- Even force distribution in hangers, and use of the same cross-section for all hangers
- Minimizing maximum force in the hangers, which reduces the cross-section area
- Reduction of the force variations in the hangers to minimize fatigue
- Aesthetic appearance.

Teich [13] investigated five different hanger arrangements based on the criteria's given above. In which he concluded that the radial hanger arrangement provides the best structural performance. The optimal force distribution does not apply for the most outer hangers. They have to be manually configured for each case.

Radial hanger arrangement was developed by Brunn and Shanack [15] and are based on the idea that no bending moment will occur if the force is transferred radially to the arch when it has a circular shape. This can be achieved by a symmetrical loading around the radius of the curvature for the respective pair of hangers.

The radial hanger arrangement has the following criteria's, see figure 3.12.

- Top hanger nodes are placed equidistantly (d) along the span of the arch. This ensures that only small local deformations occur in the arch when load is applied over the whole span [8].
- The hangers are tilted with the same angle (α) over the whole curvature of the arch.

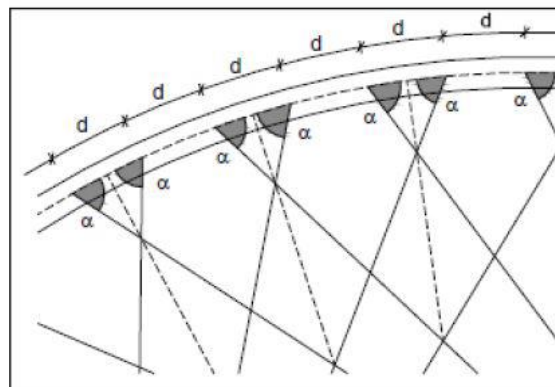


Figure 3.12: Radial hanger arrangement [15].

Furthermore, guidelines are used to determine number of hangers and inclination angle for a given bridge span, see figure 3.13. The maximum number of hangers should be limited to 50 per arch, more than 50 hangers gives little, or no increase in structural performance [13].

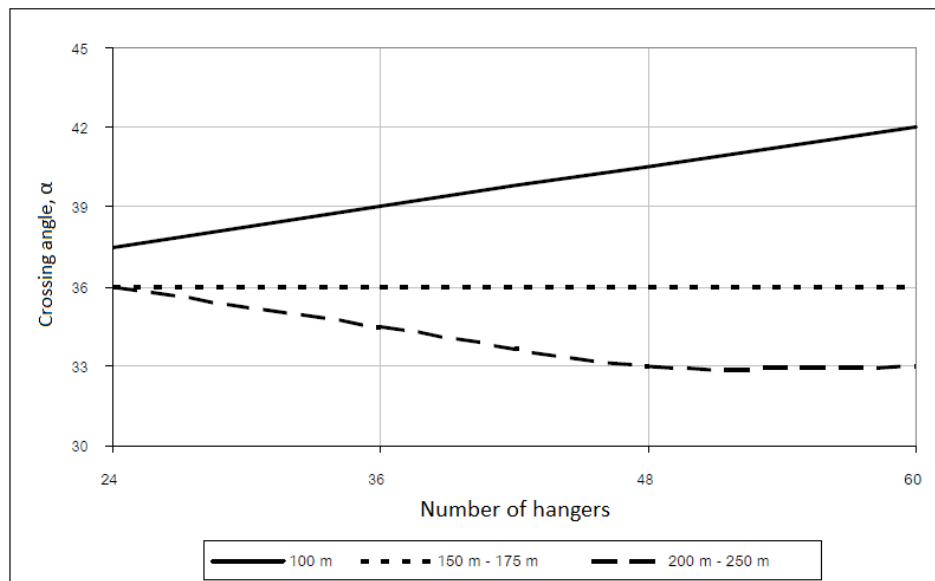


Figure 3.13: Crossing angles for different bridge spans, relevant to radial hanger arrangement [13].

3.5 Main girder and deck

The main girder transfers loads into the hangers, which again are transferred to the arch. Additionally, the main girder takes up the horizontal forces from the arches. In that way the abutments only need to withstand the vertical force components from the arch.

The distance between the bottom nodes of the hangers is decisive for the required bending stiffness of the main girder. Since the number of hangers are larger in a network arch bridge than on a tied-arch bridge with vertical hangers, less bending stiffness is required and the girders can be more slender [16].

When a load is applied to the bridge girder it is important that the load is distributed over a large area of the arch to reduce local bending moments. When the girder is relatively stiff in comparison to the arch, the diffusion of the loads happens as the girder bends, more hangers are tensioned, and this leads to a larger distribution of forces [12p. 481].

Figure 3.14 shows a comparison between a network arch bridge with low and high stiffness in the girder, the bending moment is reduced in the arch when a girder with high stiffness is chosen.

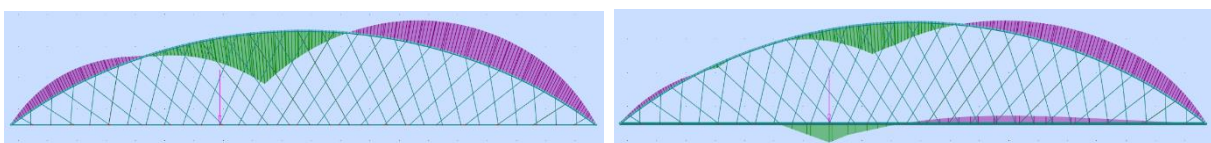


Figure 3.14: Left: concentrated load on a deck with low stiffness, right: concentrated load on bridge with high stiffness

In the research of Teich [13] he found that using a stiffness ratio higher than $\frac{I_{arch}}{I_{girder}} = \frac{1}{3}$ only gives a limited reduction of the stresses in the arch. Reduction was found to be between 3-10% depending on the slope of the hangers.

For network arch bridges Tveit [6] recommends using concrete as the lower chord, both for economic reasons, and that the tensile forces between the arches is best absorbed by prestressing cables. When the deck is designed using concrete, the edge beams is casted with the deck, and prestressing run through these beams. Transverse bending moments are often larger than in the longitudinal direction because of the small distances between hangers. When the distance between arches exceed 12 meters, transverse prestressing should be considered. If the distance between the arches are over 20 meters, transversal steel beams will be needed.

Edge beams made of steel it is often a I-section or a box-section. This makes connections to the hangers simple, even though it is not the most aesthetically pleasing appearance.

3.6 Analysis

In this chapter the geometrically non-linear analysis (GNL analysis) inputs will be highlighted. The information is important to determine a strategy to obtain valid results from the numerical analysis.

The bridges are evaluated in the structural analysis software Robot Structural Analysis (RSA). RSA is

3.6.1 Solver setup

Incremental method

As a default, the incremental method is applied in RSA when a non-linear element is used in the model. The load is divided into increments. These loads are then applied on the structure in several load steps, or iterations. The following load increment is applied once the state of equilibrium is achieved for the previous increment. Figure 3.15 explains the incremental method [17].

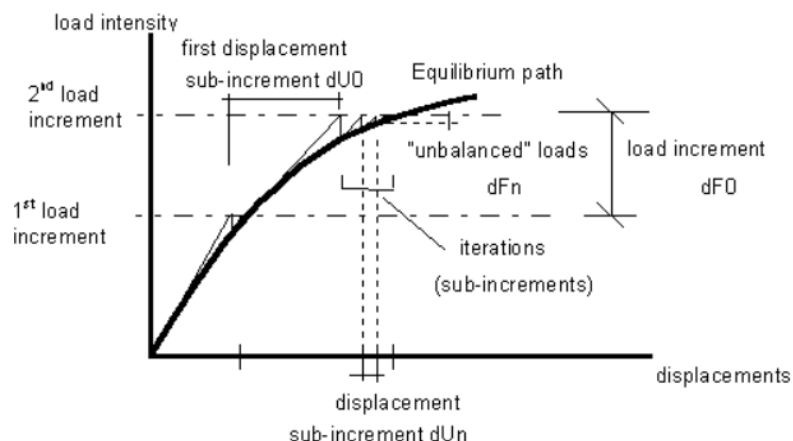


Figure 3.15: Incremental method of non-linear analysis [17].

The incremental method must be used for complex structures in cases where the impact of non-linear effects is considerable, because if the load is applied all at once it is possible that there will be no convergence of the calculations.

The default values for load increment number and maximum iteration number for one increment is 5 and 40, respectively.

Analysis process

There are three different algorithms for solving non-linear problems:

- The Initial Stress method.
- The Modified Newton-Raphson method.
- The Full Newton-Raphson method.

The methods differ in the speed of the analysis, and the probability of convergence increases when using the Full Newton-Raphson method. By default, the Modified Newton-Raphson method is chosen.

Advanced bar properties

In RSA additional properties for bars can be specified:

- Truss bars, where only axial forces act, linear analysis
- Tension or compression bars, non-linear analysis

Tension/compression bar analysis are performed the same way as for truss bars in RSA. Defining releases in the bar nodes are not possible when truss bars are selected.

-

3.7 Buckling

For a slender construction, like the network arch bridge, safety against buckling must be considered. Especially, since parts of the bridge structure are subjected to large compression forces. For network arch bridges with wind bracing there are mainly two different types of buckling that can occur.

- In-plane buckling of the arches.
- Out-of-plane buckling of the wind bracing [7p. 26].

Per Tveit [6] developed the assumption of the in-plane buckling mode shape presented in figure 3.16. This shape is only valid for a certain combination of bridge geometry and cross-sections.

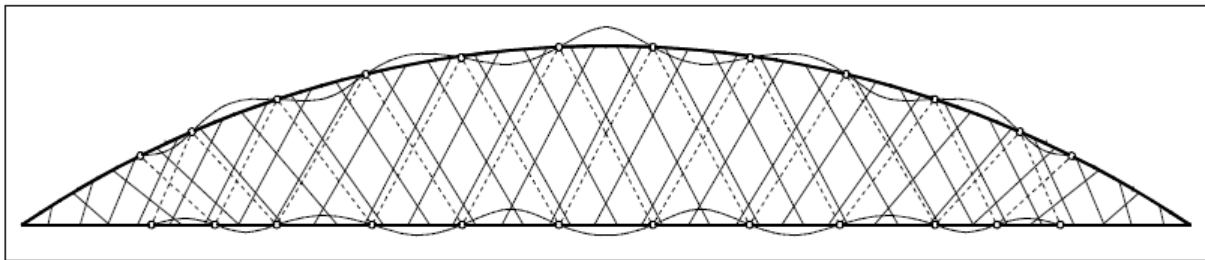


Figure 3.16: In-plane buckling of network arch bridge showing the buckling mode shape [6].

Frank Schanack [18] did a parametric study to find an analytical model that could be valid for network arch bridges with different spans, hanger angles, rise and number of hangers.

From the parametric study he concluded:

Generally, the bending stiffness of the arch has the biggest influence on the buckling load. Less important is the arch-hanger angle and the hanger numbers. Further:

1. The decisive load case is: full load over the whole bridge.
2. Buckling load increases with the number of hangers. The reason for this is that the buckling length shortens as the wave crests of the buckling mode shape increases, which is the case for an increase the number of hangers.
3. For the hangers he used radial hanger arrangement and found that steeper hangers give larger resistance against buckling.
4. The tie may be considered as bending stiff.

As the tie reaches a certain moment of inertia, where it may be considered totally stiff compared to the arch and hangers, no further increase of the moment of inertia leads to an increase of the buckling load.

5. By studying different moments of inertia for the arch, Schanack found that, according to Euler's buckling theory the bending stiffness of the arch has a lot of impact on the buckling load and that larger bending stiffness increases the buckling load. Considering all the parameter variations this has the largest influence of the buckling load.
6. The critical mode shape is a wave-like deformation of variable order.

No study was done on the effect of the arch curvature on the in-plane buckling load.

As described earlier the in-plane stability of the network arch bridge is generally better than tied arch bridges because of the supporting effect of the inclined hangers. This is if an optimal hanger arrangement is chosen, so that no relaxation of any hangers occur [16].

3.8 Moving loads

3.8.1 Envelopes

When a bridge is subjected to multiple loading scenarios like live loads it can be hard to identify the position on the bridge that gives the largest stresses; whether it is moment, shear, axial force or deflection. Envelopes can be used for this. For example, for bending moments on a bridge as a result of a moving load. All the moment diagrams for the different load positions of the vehicle are compiled together, and only the location giving the largest moment in a given point is presented [19].

3.9 Construction of network arches

Steel bridges are prefabricated structures which are assembled/welded together at the construction site. Close attention to detail is very important because of all the welding that goes into the structure, by doing this under controlled conditions at a manufacturing plant a lot of potential errors are prevented.

Arches are produced in segments, with the hanger connections being welded to each segment at the plant.

4 Research question

For a structure like the network arch bridge there are many areas that could be investigated in this master thesis. During literature study for the pre-project little work about the optimization of the bridge arch was found. After meetings with the supervisors at UiA we agreed that the thesis should be about the problems around the arch end. When using a circular shape for the arch the moments tend to rise at this area. A reduction of the radius at the bridge end will lower the moments. Based on that the following research question was formed:

“How can the optimal curvature of a network arch bridge be obtained?”

4.1 Sub questions

To break down the research question into more manageable parts the following sub questions was formed:

- “How will different curvatures effect the moments at the arch end?”
- “What kind of arch shape will improve the structural behavior most?”

5 Method

The experimental method is based on changing only one variable at a time. By looking at, and changing one variable at a time, the results can be directly attributed to the independent variable. In that way it is possible to conclude whether this variable has an impact on the results or not. The different variables that is considered in this thesis are given in chapter 6.2. Parameters like loads, cross-sections, materials, supports and releases should be constant for all models to prevent misinterpretation of results.

This chapter will give an overview of how the results were obtained by using numerical modeling and calculations.

5.1 The arch geometries

Based on the knowledge from the literature study on different arch shape it was decided that three different types of arch geometry would be interesting to investigate further. These three shapes are presented in the following chapter.

5.1.1 Circular arch

The first geometrical shape is the arch that is part of a circle. That means that the arch will have the same radius over the whole bridge span. Optimizing the curvature of the network arch bridge is based on this shape because most network arch bridges built today uses this curvature. A description of the circular arch is given in figure 6.1.

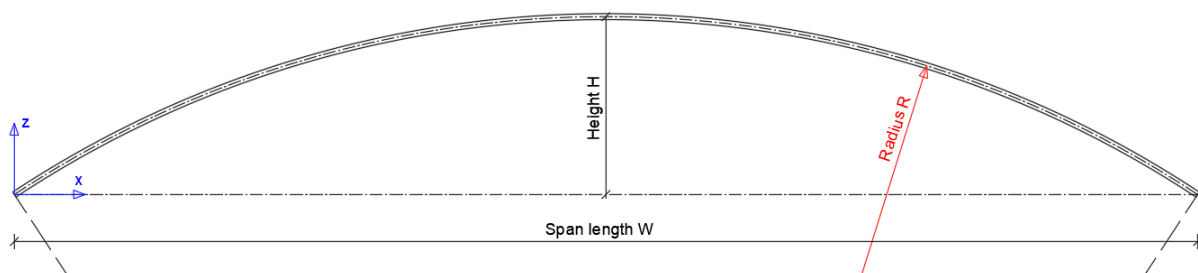


Figure 5.1: Circular arch shape [own figure].

5.1.2 Elliptical

One of the alternative curvatures is a shape that is part of an ellipse. For this shape the arch radius varies over the whole bridge span.

The elliptical arch is defined by the large radius (r_a) and small radius (r_b) which can be seen in figure 6.3, this figure also shows the range that is used for the elliptical arch.

Analysis is carried out with different ratios between r_a and r_b . The ratios are defined as $\frac{r_b}{r_a}$.

The respective radiuses are obtained by using the radius formula (6.1) that

Teich [13, p. 237] presents in his thesis. Given parameters in the formula are the bridge length and the arch rise:

$$r_a = \frac{r_b \times W}{2 \times \sqrt{2 \times r_b - H} \times \sqrt{H}} \tag{6.1}$$

Where:

W Bridge length.

H Arch rise.

The elliptical arch shape with its geometry is given in figure 6.2.

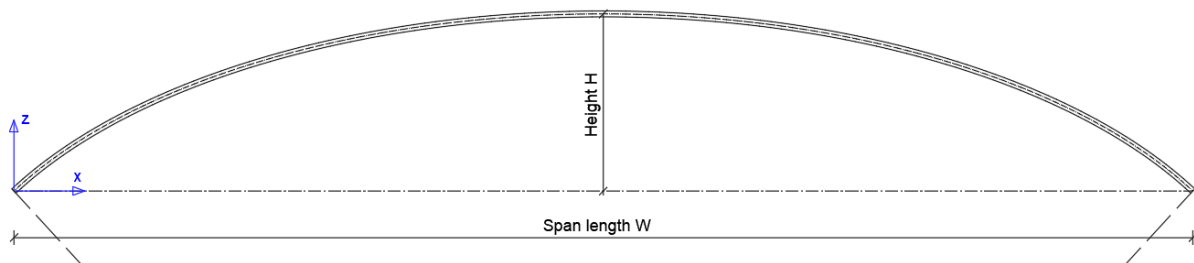


Figure 5.2: Elliptical arch shape [own figure].

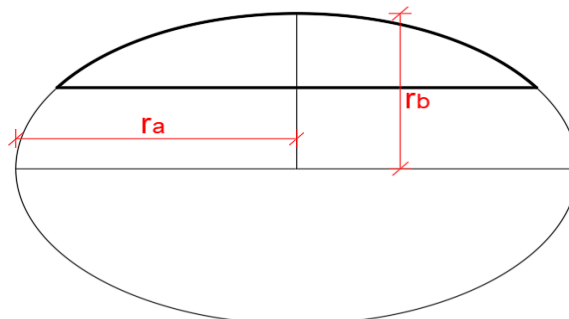


Figure 5.3: Relation between r_a and r_b , outlined region represents the used range for the bridge [own figure].

5.1.3 Three-center arch (TCA)

Brunn and Shanacks [15] research on reduced radius at the wind portal were based on the following geometry. An arch consisting of two different radiuses. One radius for the main part of the arch (R) and one with reduced radius (r) at the end of the bridge on both sides. The ratio between the two radiuses are given as, $\frac{r}{R}$.

In this thesis two different configurations of TCA are investigated:

- In figure 6.4 H , W and w remains unchanged regardless of the radius ratio.
- In figure 6.5 W , H and h remains unchanged regardless of the radius ratio.

The reasons for comparing these two configurations is that they have different advantages. The arch in figure 6.4 has a fixed length, w . For constructional reasons it might be required that the transition point where the two curvatures meet should be placed at a certain distance in z -direction.

For the arch in figure 6.5 the height, h is fixed. This configuration can be used in cases where the transition point is placed at a certain distance in x -direction.

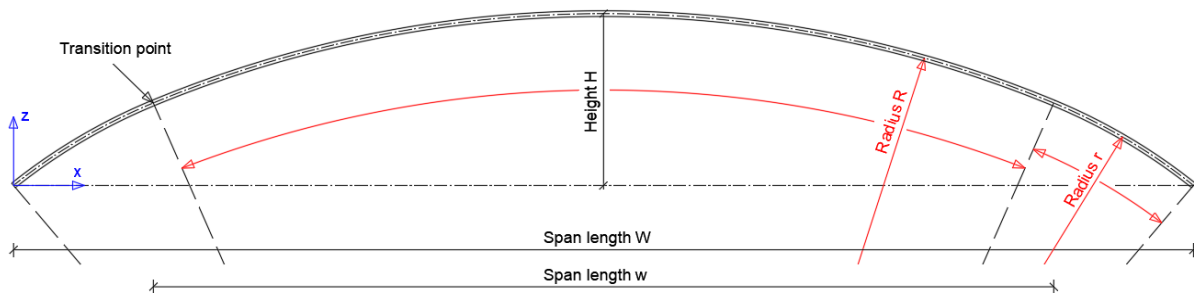


Figure 5.4: Three center arch where span length, w is constant [own figure].

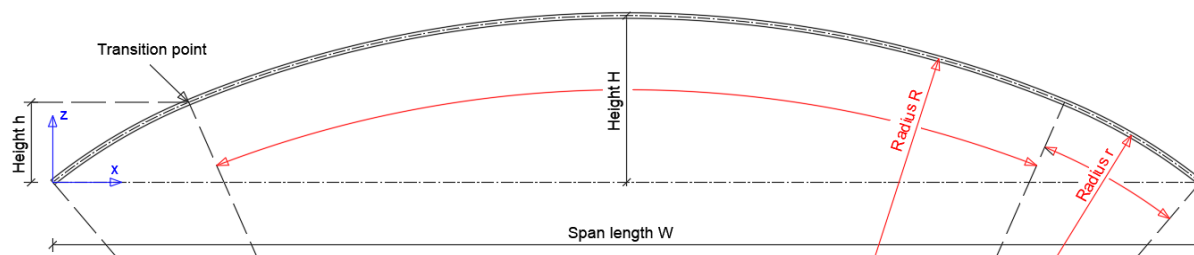


Figure 5.5: Three center arch where height, h is constant [own figure].

Obtaining the geometry:

To obtain the right geometry the challenge was to find an equation to describe the length of the bridge, W. Figure 6.6 shows the sketch used to find the arch geometry when h is fixed.

This was done by finding an equation for the length, x (distance from the origin to the transition point). Then, the point (a,b) could be expressed, and finally an equation for W. Equations are given in table 6.1. In appendix E the expressions used to find the curvature when w is fixed are given.

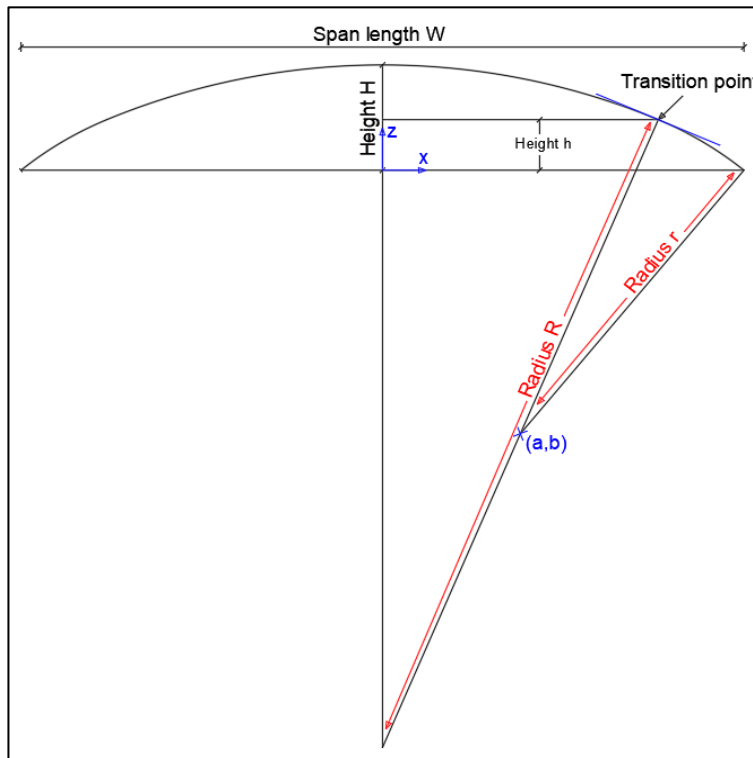


Figure 5.6: Sketch used to obtain the expression for W [own figure].

Table 5.1: Equations.

Expression for x (distance from origin to the transition point)	Expression for a	Expression for b	Expression for the bridge span, W:
$x^2 = R^2 - (h - H + R)^2$ $x = \sqrt{R^2 - (h - H + R)^2}$	$a = x \times \frac{(R - r)}{R}$	$b = h - r \times \frac{(R - H + h)}{R}$	$W = 2 \times (a + \sqrt{r^2 - b^2})$

Further the radiuses could be found by using the Goal Seek function in Excel. Goal Seek uses an approach where it back-solves a problem by plugging in guesses until it arrives at an answer. In this case it was used to find out how much the large radius, R must change for the length, W to be 200 meters.

It is worth mentioning that the formulas had to be deduced so that the tangents of the two radiuses coincided at the transition point. Any small change in angle at this point would lead to an increase of stresses.

Strategy

The strategy for analyzing the different arch geometry with different radius ratios. After a set of parameters is defined the structure is analyzed with different radius ratios. The ratio starts at 1.0 (circular shape) and are reduced with increments of 0.1. As the theory states it is expected that the decrease of bending moment will stop at a given ratio. This ratio is set to 0.3.

This is done by using the formulas given in table 6.1 for the TCA models and equation (6.1) for the elliptical arches in excel.

AutoCAD is then used to draw 2D-models of each case. Further the models are imported into RSA for analyzing.

5.2 Geometries

Different variables are changed to see if this effects the structural behavior when the radius ratios are reduced. In table 6.2 and 6.3 the different models are shown. As can be seen, only one variable is changes at a time.

Table 5.2: Models for TCA.

Model	Rise [m]	Length [m]	Hanger inclination [α]	Transition point [m]	Number of hangers
1	30	200	30	h constant: 14,4	50
2	30	200	30	w' constant: 80	50
3	30	200	40	h constant: 14,4	50
4	34	200	30	h constant: 14,4	50
5	30	200	30	h constant: 14,4	48

Models that have the same arch geometry: Model 1, 3 and 4.

Table 5.3: Models for elliptical arch.

Model	Rise [m]	Length [m]	Hanger inclination [α]	Number of hangers
6	30	200	30	50
7	34	200	30	50
8	30	200	30	48

Models that have the same arch geometry: Model 1 and 2.

Further on the different cases will be referred to by its model number.

5.2.1 Explanation of variations

Length

The length of was decided to be constant at a length of 200 meters.

Rise

A rise of 30 and 34 meters are used because it represents the range of the ideal height of a network arch bridge. 15 and 17 % respectively, when a bridge span of 200 meters is considered.

Hanger inclination

Two hanger inclinations where chosen for TCA, 30 and 40 degrees. As chapter 3.4.2 states the optimal angle for a bridge-span of 200 meters is 33 degrees. It was chosen to look at 30 degrees for ease of modeling, and 40 degrees for comparison.

Transition point

This is only chosen for TCA. A height $h=14,4$ meters was chosen based on the example case in the thesis by Bruun and Schanack, where: $h = 0.48 \times span = 0.48 \times 200 m = 14,4 m$ [15].

The distance w' for model 2 was chosen to be 80 meters. This gives a height (h) of 11,46 m for the transition point in model 2 with no reduction of radius. As this is about 3 meters lower then 14,4 m comparisons on the effect of where the transition point is placed, can be discussed.

Number of hangers

As there is no increase in structural performance with more than 50 hangers per arch, 50 hangers where chosen. For comparison 48 hangers where chosen.

5.3 Modeling

5.3.1 AutoCAD

After the ratios has been found for the respective arch geometries, the models are drawn in AutoCAD. The reason for this is that a complex structure like a network arch bridge is hard to model directly in RSA. Thereafter, the models are imported into RSA for further analyzes

5.3.2 Robot Structural Analysis (RSA)

Inputs

When importing the AutoCAD model into Robot number of arc discretization's must be chosen. This is because Robot turns continuous arc element into discrete elements. When the number of elements is higher, the better it simulates the true arc shape. The graph below shows an arch spanning 200 meters with a rise of 30 meters (base case for modeling), the bending moments flattens out at a certain value as the number of elements increases. To speed up the analysis, the least number of elements that gives correct answers are preferable. Therefore, an arc discretization of 185 elements are chosen for all the models, see figure 6.7.

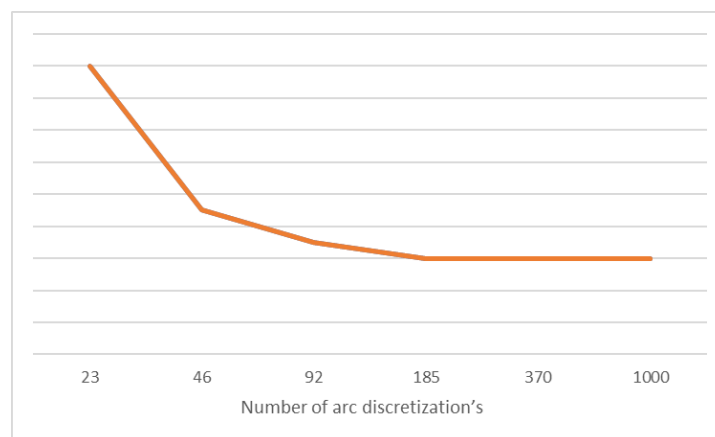


Figure 5.7: Number of elements used in numerical calculations [own figure].

Material data for the super structure are given in the table below.

Table 5.4: Material types.

Type	Material	Cross-section	Moment of inertia [mm ⁴]
			I _z
Main girder	S420 M/ML	IPE 600	3,387E+07
Main girder buckling ⁽¹⁾	S420 M/ML	IPE 800	1,129E+08
Hangers	S420 M/ML	d = 60 mm	-
Arch ⁽²⁾	S420 M/ML	KR 600x40 mm	2,773E+08

- ⁽¹⁾ A fictitious cross-section which purpose is to increase the in-plane bending stiffness of the main girder.
- ⁽²⁾ Also, a fictitious cross-section to secure large bending stiffness both in-plane.

Boundary conditions

The models are supported as pinned at one end and pinned with free translation in x-direction at the other end.

Hangers

The hangers are modelled as non-linear tension bars. This makes for a more realistic modeling as the hangers in a network arch bridge cannot take any compression forces.

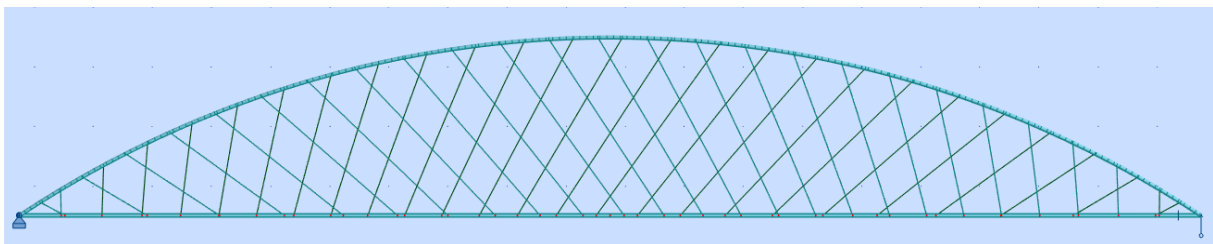
Buckling

The basic result of a buckling analysis gives critical coefficients (eigenvalues). The critical coefficient is the factor that the applied load should be multiplied with to obtain appropriate loss of stability.

In Robot number of analyzed modes are selected before calculations. Outputs of critical coefficients can often be negative in Robot. These are values that implies that the applied load should be placed in the opposite direction for the given buckling mode to occur. The negative values should therefore be neglected and the first positive value appearing is the critical coefficient of the structure that should be investigated. The problem is that it may result in the unavoidable job to calculate a lot of critical coefficients before the first positive one occurs. When analyzing the different models, number of modes was set to 20 to ensure that one positive value would appear.

Two-dimensional model

The first step is to analyze the different arch geometries using a two-dimensional model in RSA, see figure below.



After the results from the 2D-models are analyzed, three models are further investigated. These models will have the same basic geometry. TCA and the elliptical arch will be analyzed with their respective radius ratio that gives the best structural improvement.

- Model A: Circular arch.
Geometry: Length = 200 m, H = 30 m, $\alpha = 30^\circ$
- Model B: TCA with the optimal radius ratio based on the results from the 2D analysis.
Geometry: Length = 200 m, h = 14,4 m, H = 30 m, $\alpha = 30^\circ$
- Model C: Elliptical arch with the optimal radius ratio based on the results from the 2D analysis.
Geometry: Length = 200 m, H = 30 m, $\alpha = 30^\circ$

Loads

As this thesis does not focus on design of network arch bridges the specific design loads on the bridge is not of importance. Only simple loads will be applied on the different bridge models, as it is the comparison between the results that are of importance, not the values themselves. Self-weight of the bridge models is neglected as the weight will be different every time one geometrical change is done to the structure, this can affect the results.

Two load combinations (table 6.5) were used to analyze the different models, application of the loads is shown in figure 6.8.

Table 5.5: Load combinations.

	Dead load	Load [kN/m]	Live load	Load [kN/m]
Load combination 1	Full span	1	Full span	1
Load combination 2	Full span	1	Half span	1

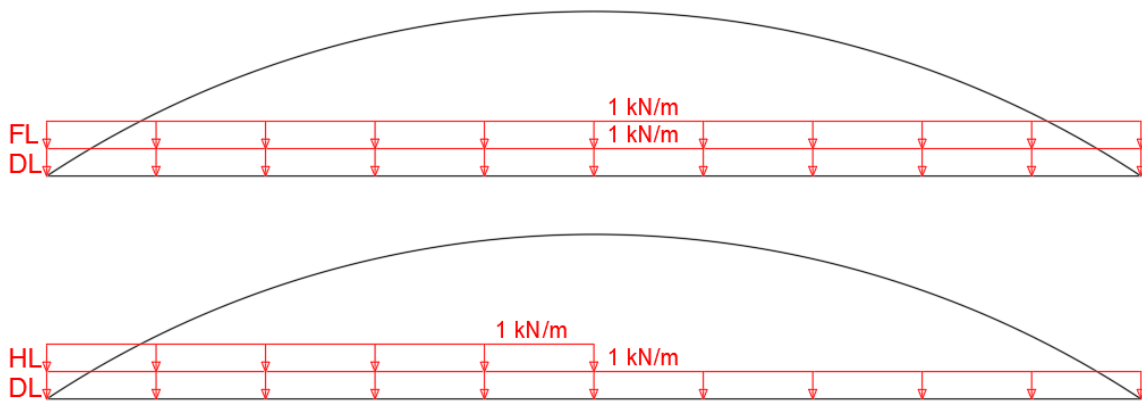


Figure 5.8: Applied loads [own figure].

When analyzing moving load on the bridge deck. Vehicle is replaced with a concentrated unit load with magnitude of 1 kN. The load is applied in steps of 2 meters along the tie.

Non variables

To narrow in the analyzing process some parameters was set to be constant for all the models. The bridge span is 200 meters. For the hangers, radial hanger arrangement is used. One problem arises with this, and that is when the ratio gets low and the curvature of the arch at the end of the bridge gets almost vertical. For those cases the hangers had to be manually adjusted to the tie. The distance between the top nodes stays constant. An example of this can be seen in figure 6.9.

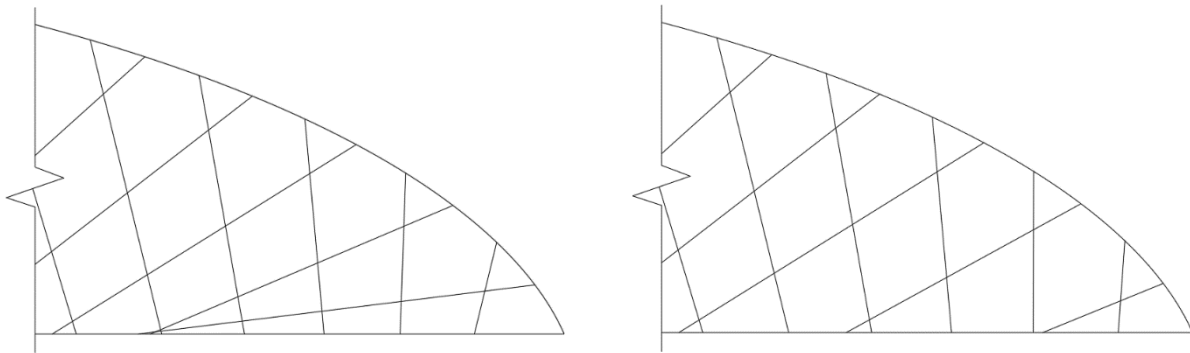


Figure 5.9: Adjustment of hangers at bridge end. Left: before, right: after [own figure].

Outputs

The following outputs will be of interest after analyzing the two-dimensional models:

- Global extremes of bending moments in the arch, both positive (underside of the arch) and negative (upper side of the arch).
- Global extremes of axial forces in the arch.
- Largest tensile force in the hangers, and number of relaxed hangers.
- Critical coefficients for comparison of in-plane buckling resistance.

For the comparison of the optimal arch shapes the following outputs will be of interest:

- Buckling mode shape with critical coefficient.
- Bending moment envelope for moving load.
- Global extremes for bending moment, axial force and hanger force.

5.4 Weakness with the method

As this method is based on a lot of modeling, one improvement could have been to develop a code to obtain plot for the bridge geometries easier. A broader number of cases could have been looked at, and increments between radio ratios could have been smaller, to obtain more accurate results.

3D-models should have been used to further investigate the bridges with optimal radius ratio. Combinations containing wind loads and moving loads should have been carried out. In the wind portal of the bridge, large out-of-plane moments can occur. It would have been interesting to carry out an analysis for the different arch shapes here.

6 Results

In this chapter the results from analyzing the different arch shapes with all its models are presented. Basis for calculations refers to the appendix for each sub-chapter.

6.1 Bending moments TCA

6.1.1 Positive bending moments

Two-dimensional analysis in RSA gave the following results for the bending moments in TSA. Figure 7.1 and 7.2 show the percentual reduction of positive bending moment in the arch for the different radius ratios. Figure 7.1 indicates the reduction when full unit load applied on the bridge deck. It can be seen from the graph that the bending moment is at its lowest when the radius ratio is at 0.4 for all cases except for model 4 where the reduction seems to be far less than for the other cases. Lowest bending moment can be found for model 1 and 5 with a reduction of 39 percent. See appendix B-1 for values.

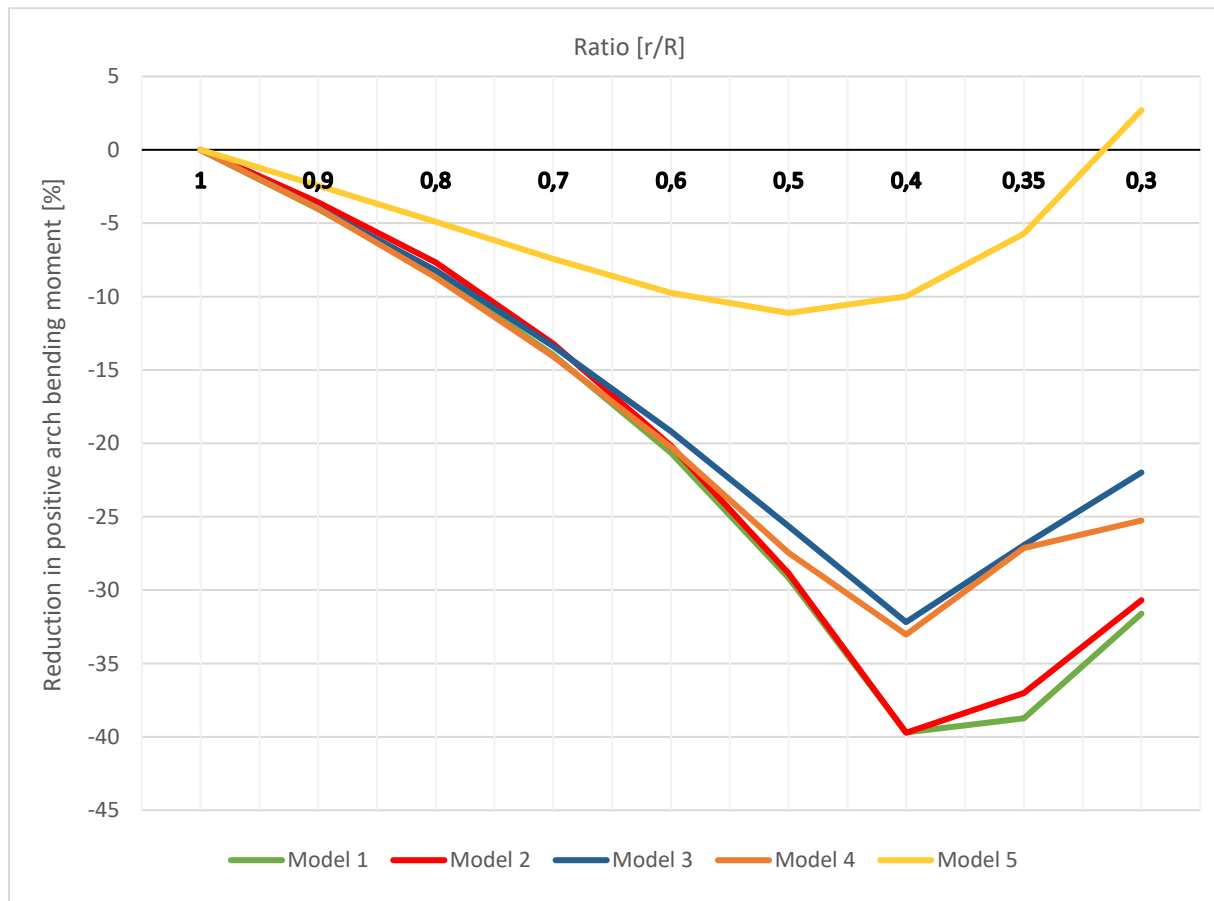


Figure 6.1: Full load.

The results are quite similar for the bending moments under half load, figure 7.2. Here, some of the models have their lowest bending moments at ratio of 0.35. Still, model 1 and 5 has the largest reduction of around 40 percent.

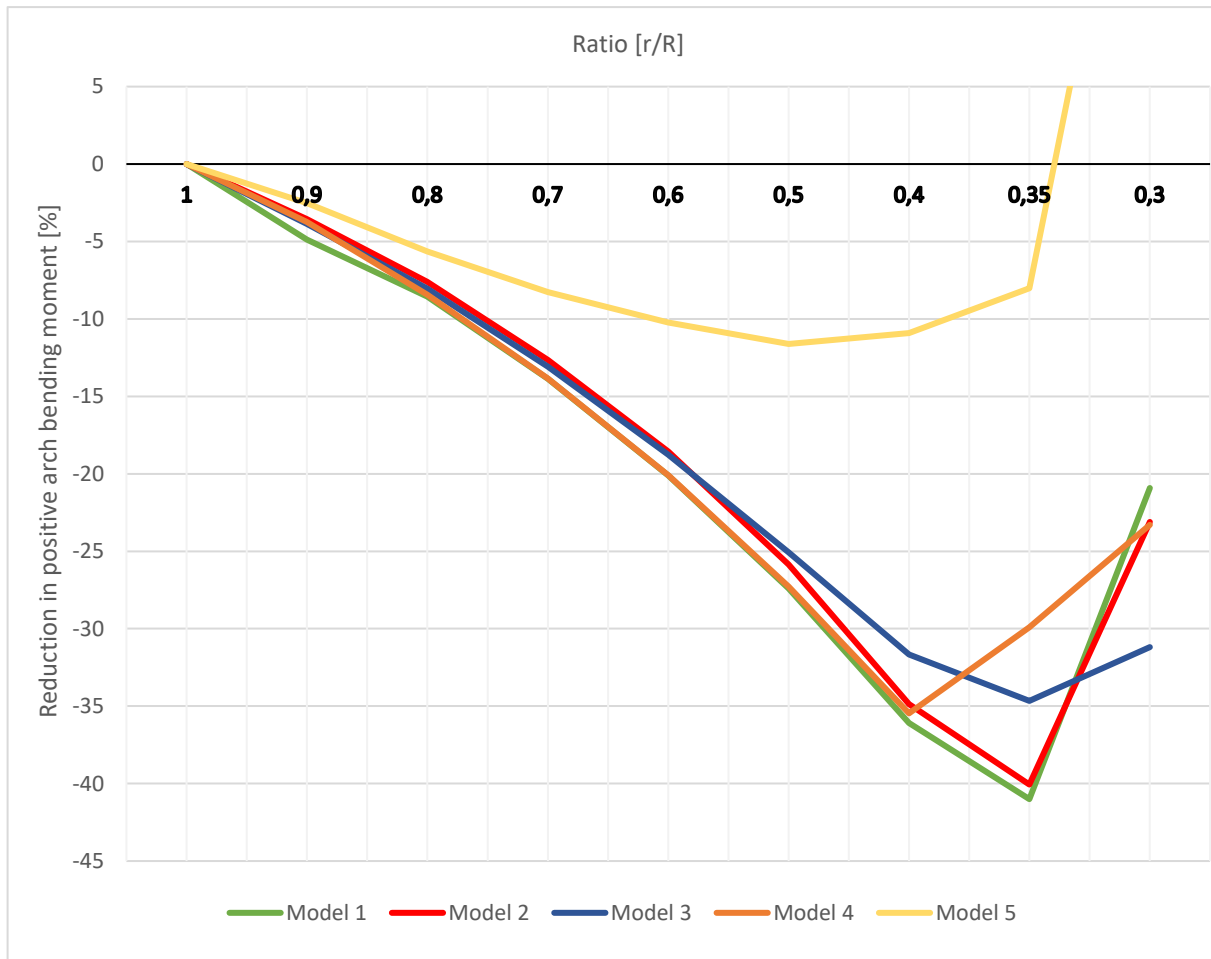


Figure 6.2: Half load.

6.1.2 Negative bending moments

Figure 7.3 shows the increase of negative bending moments in the arch when full load is applied. The vertical axis shows the actual bending moments with the applied unit loads. The radius ratio where the bending moments start to increase is the most important to look at. It shows that the increase happens between ratio 0.7 and 0.6 for all the 5 models.

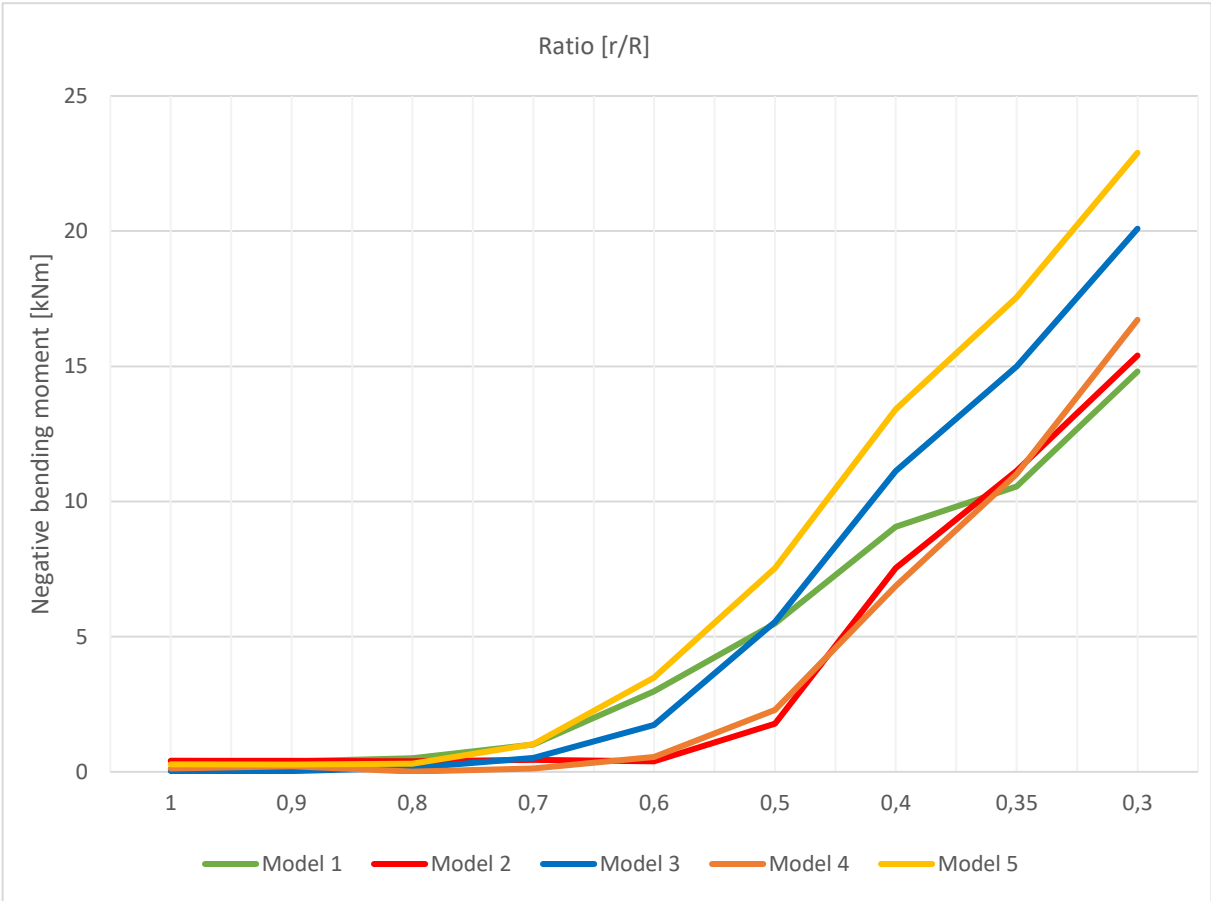


Figure 6.3: Full load.

Negative bending moments starts to arise between ratio 0.6 and 0.5 when half load is applied, see Figure 7.4. Especially case 1, 2 and 5 has a large increase below ratio 0.4.

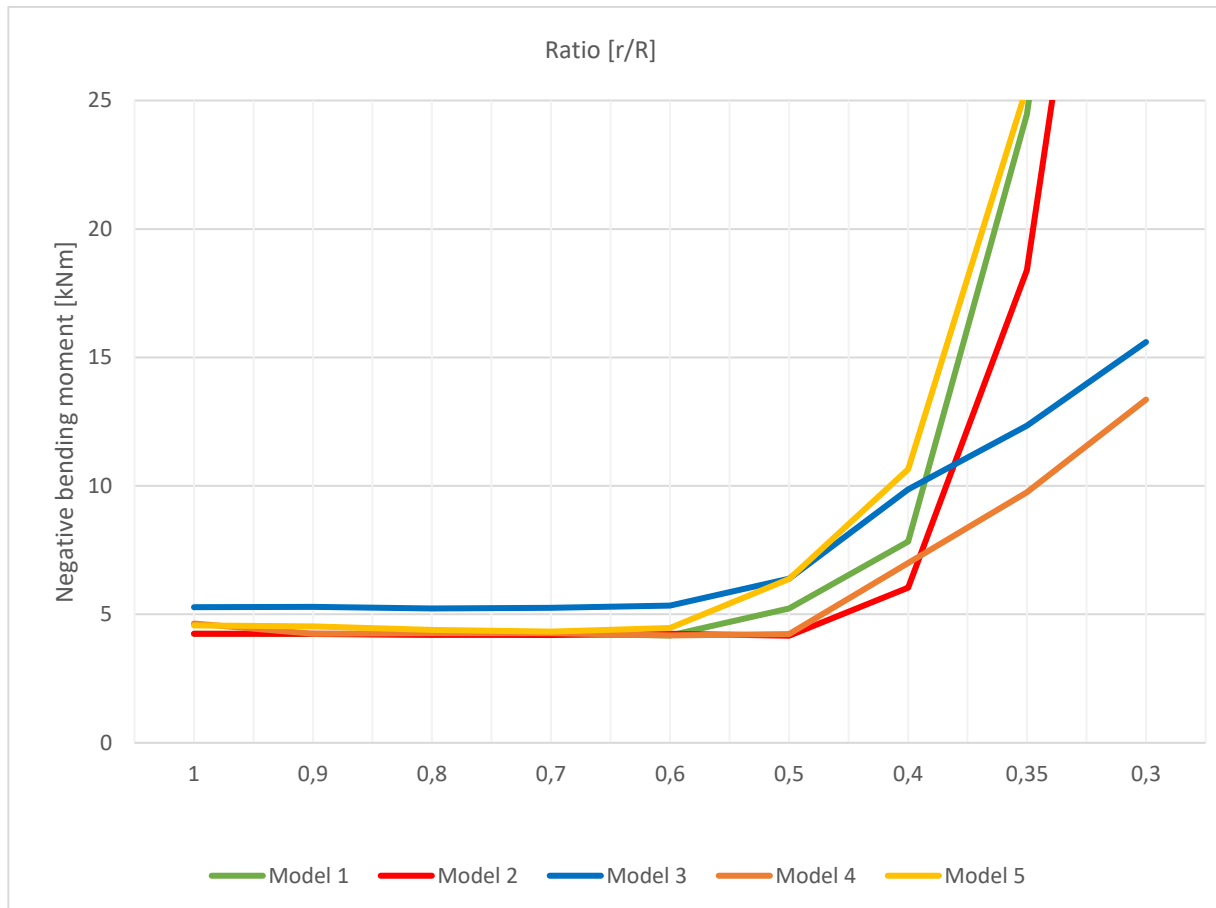


Figure 6.4: Half load.

6.2 Axial forces TCA

Figure 7.5 illustrates the percentile reduction in axial force for the different model of TCA when full load is applied. Model 3 and 4 stand out from the others. Model 3 with a reduction at ratio 0.3 of little over 1 % and model 4 with a reduction higher than 7 %. It can be seen from the figure that the reduction of axial force flattens out as the ratio decreases. See appendix B-2 for values.

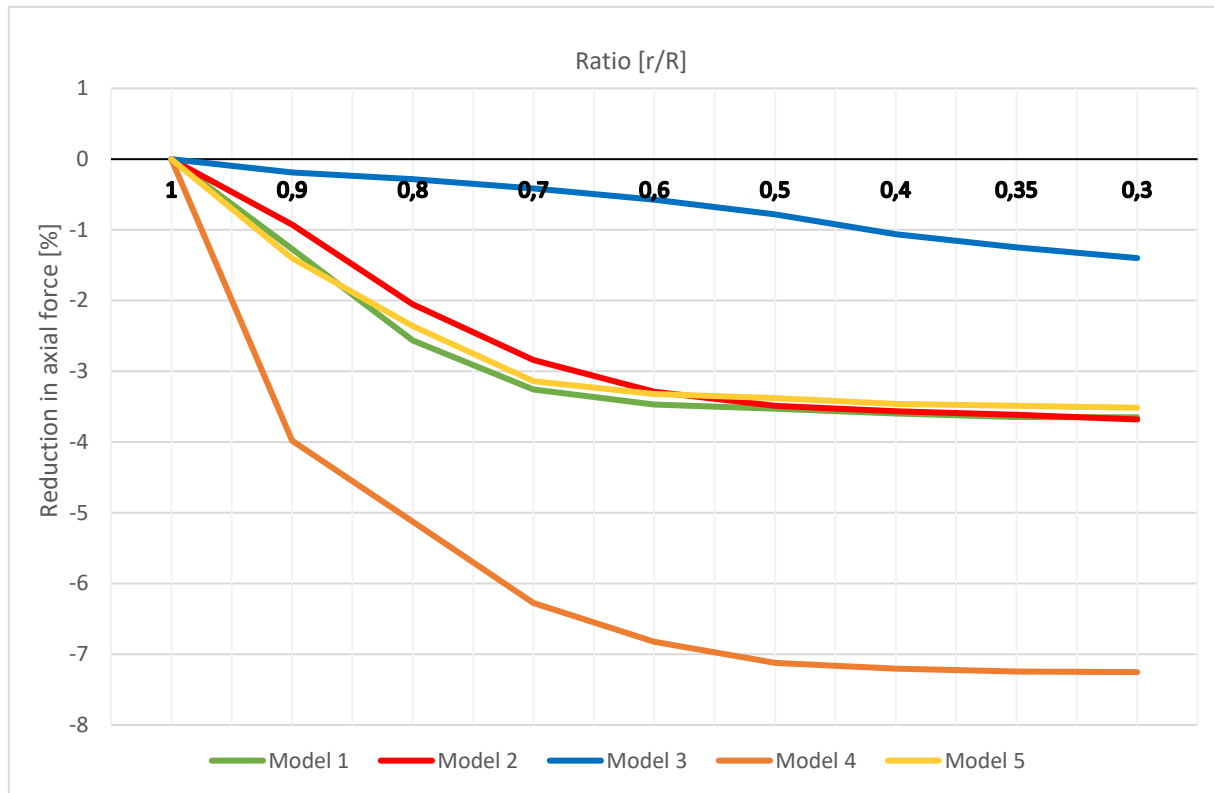


Figure 6.5: Full load.

When half load is applied there is a resemblance in the reduction of axial forces. All the models have decreased axial force of 7-10,5 % at ratio 0.3, see figure 7.6.

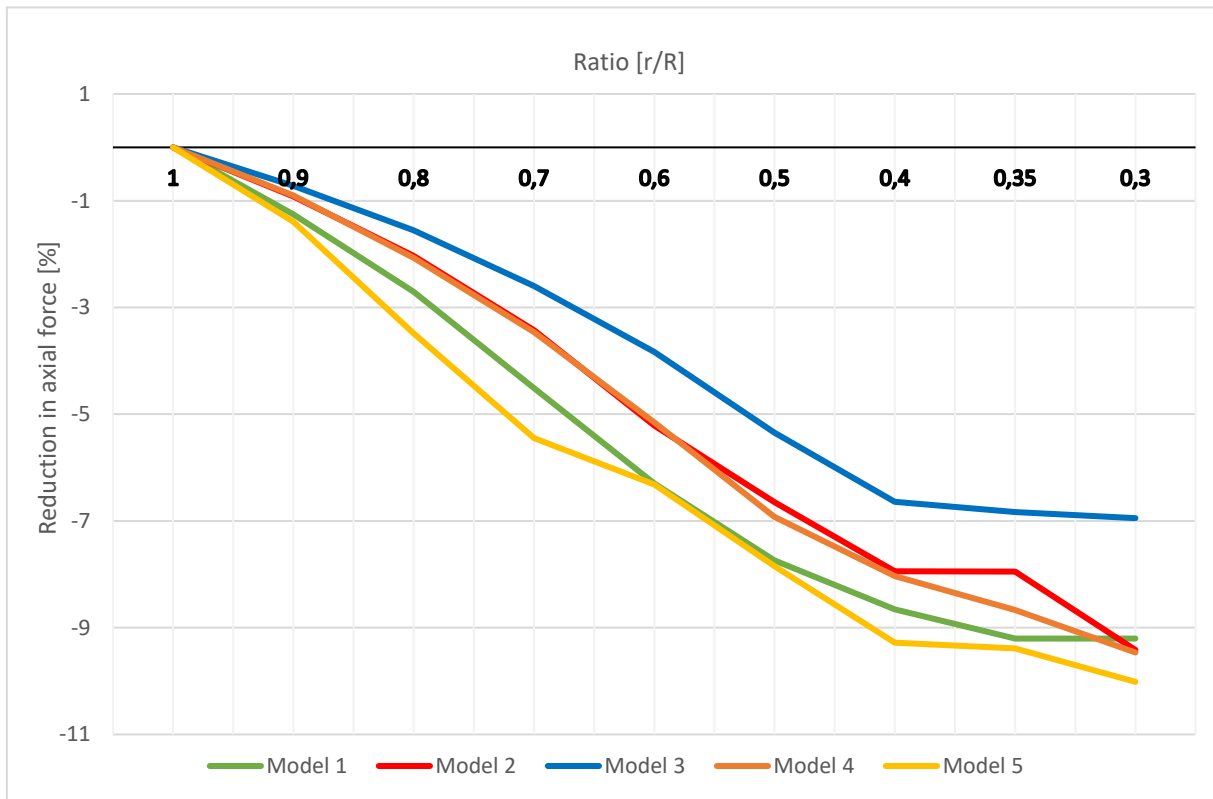


Figure 6.6: Half load.

6.3 Bending moments ellipse

6.3.1 Positive bending moments

The results from the elliptical arch models applied with full load are illustrated in figure 7.7 the positive bending moments decreases for all the modes and has its lowest point at ratio 0.5-0.4. Mode 6 decreases the most at 51 percent. Mode 8 with 48 hangers has less reduction. See appendix B-1 for values.

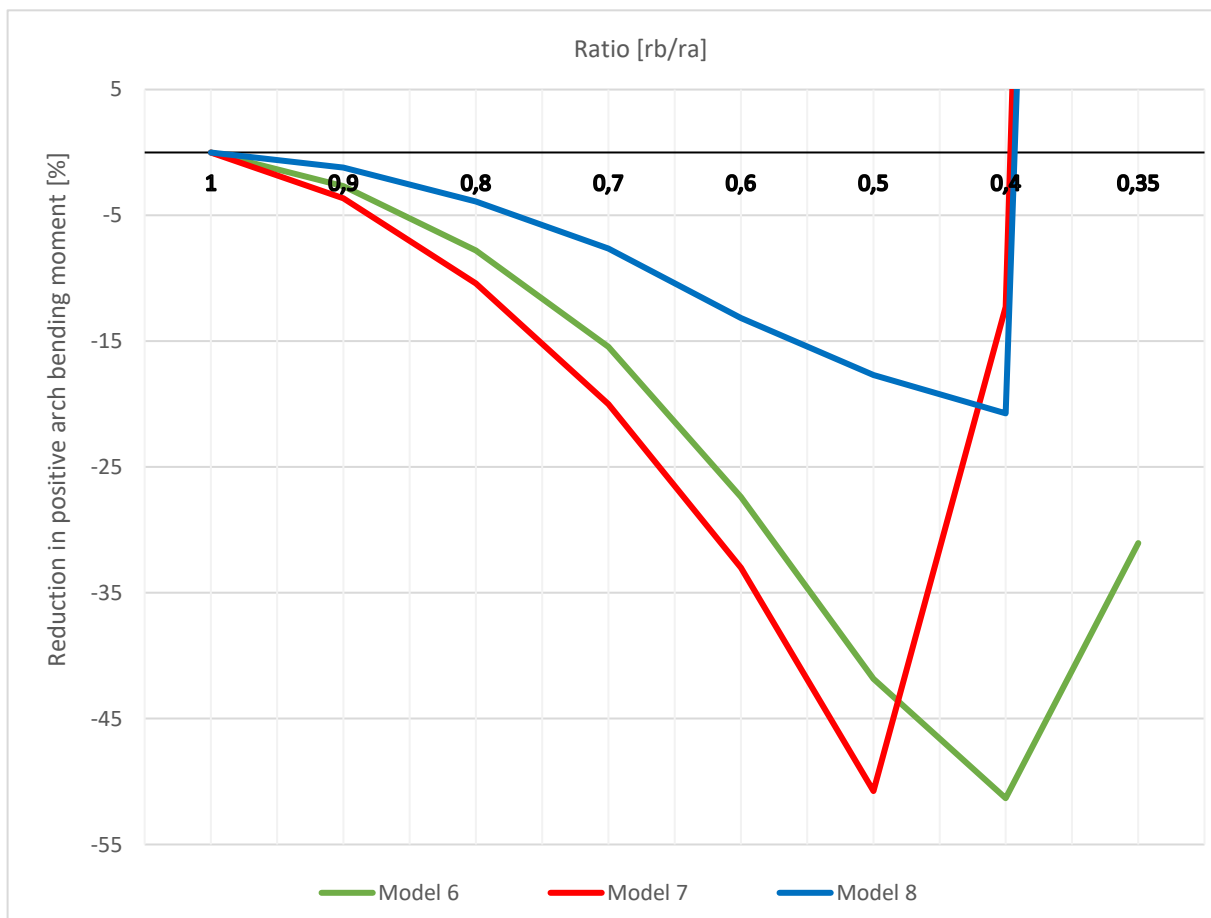


Figure 6.7: Full load.

Figure 7.8 illustrates the decrease of positive bending moment for the elliptical models when half load is applied. All modes have their lowest bending moments for ratio 0.5.

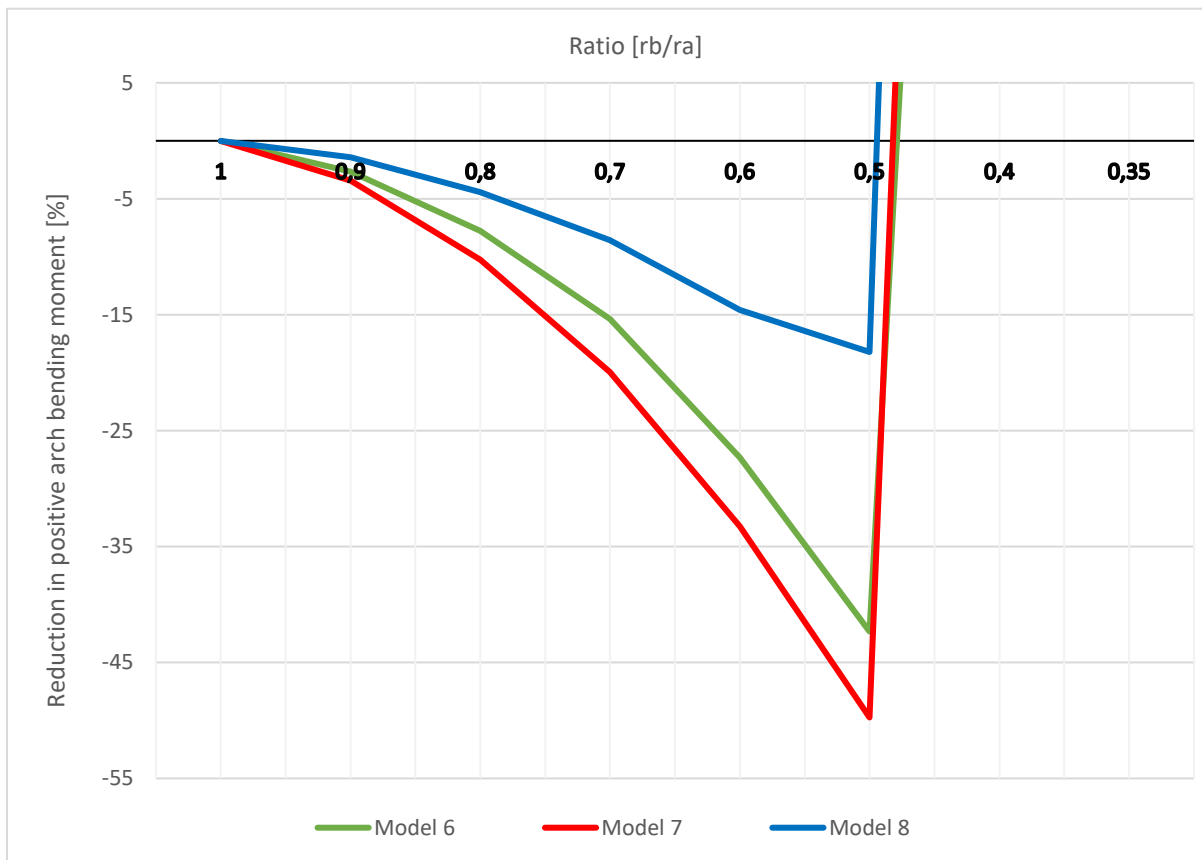


Figure 6.8: Half load.

6.3.2 Negative bending moments

For the elliptical arches the negative bending moments rapidly increases between ratio 0.7 and 0.6, see figure 7.9. All the models follow more or less the same path.

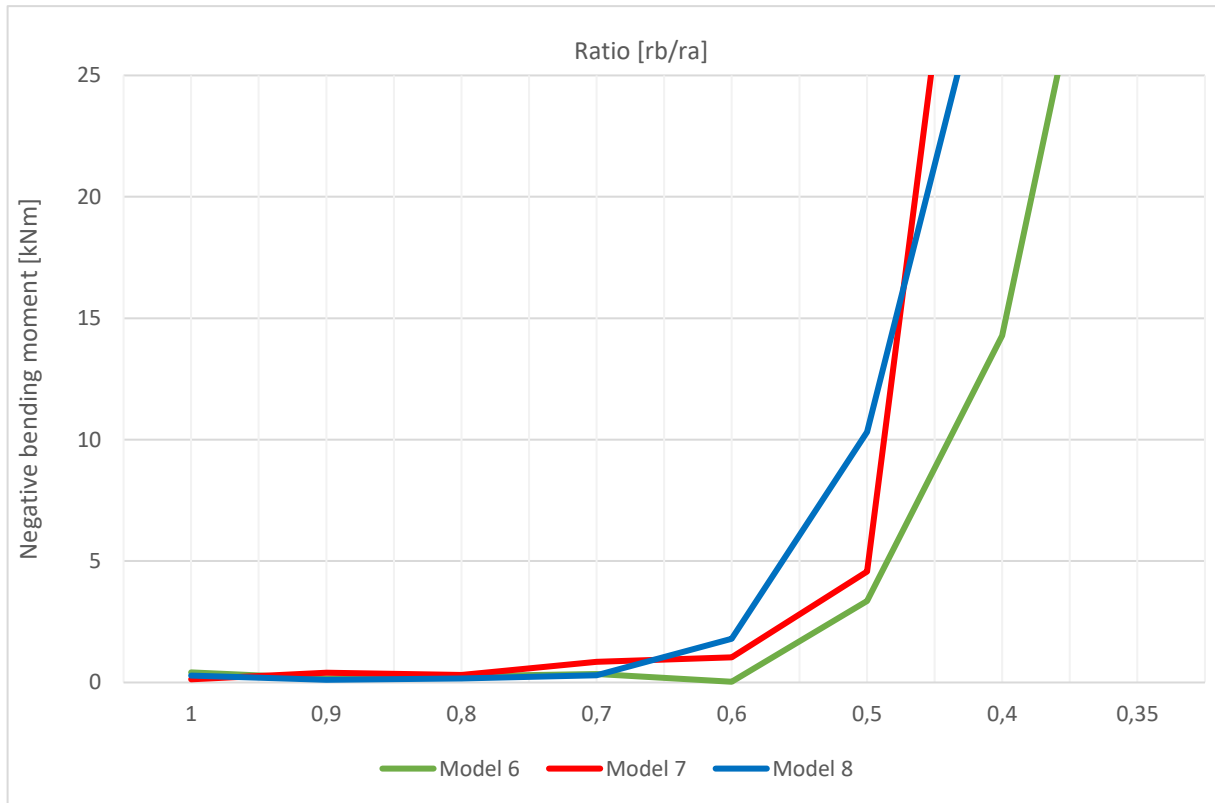


Figure 6.9: Full load.

For the half-loaded load combination there is almost no distinction of the three cases. As seen in figure 7.10 the negative bending moments start to increase at ratio 0.6 and has an almost vertical increase at 0.5.

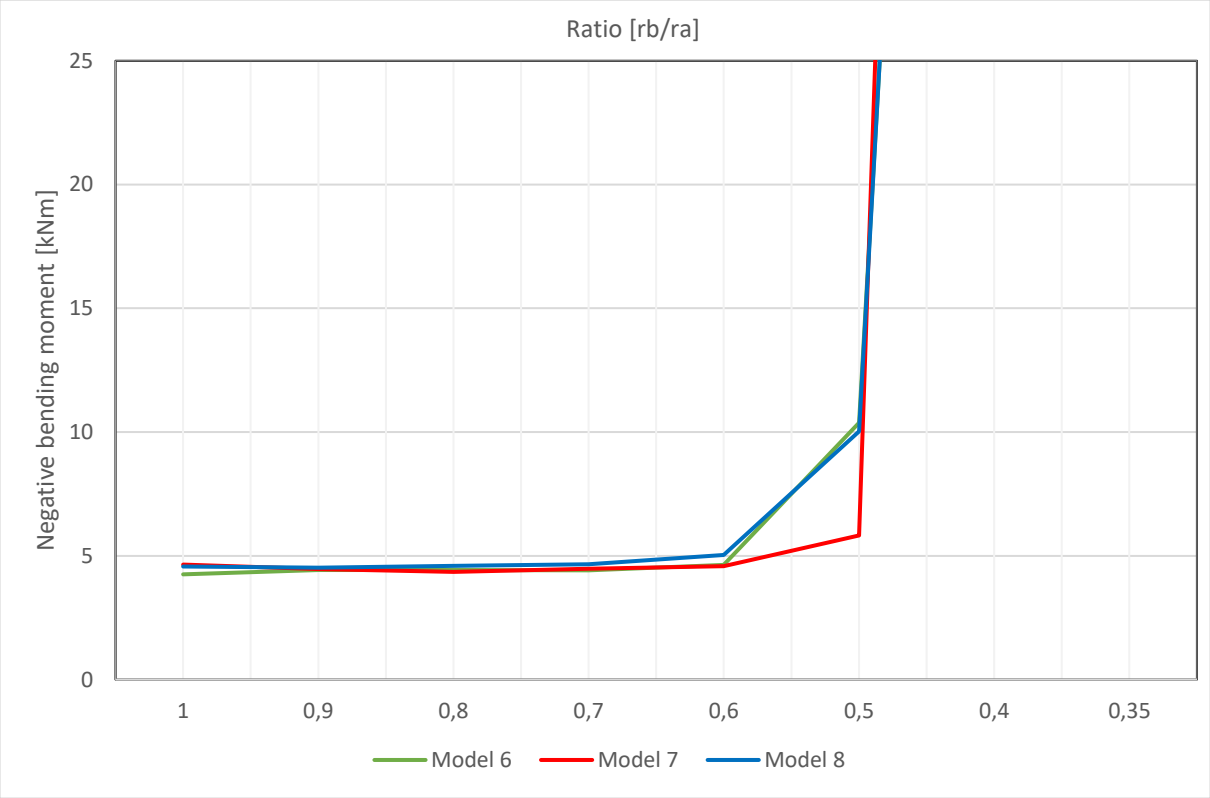


Figure 6.10: Half load.

6.4 Axial forces ellipse

For full load the axial forces decrease as the radius ratio gets smaller. Model 7 shows a larger reduction at around 8 %, but there is a tendency for the axial forces to increase between ratio 0.4 and 0.35, this also shows for model 8, see figure 7.11. See also appendix B-2 for values.

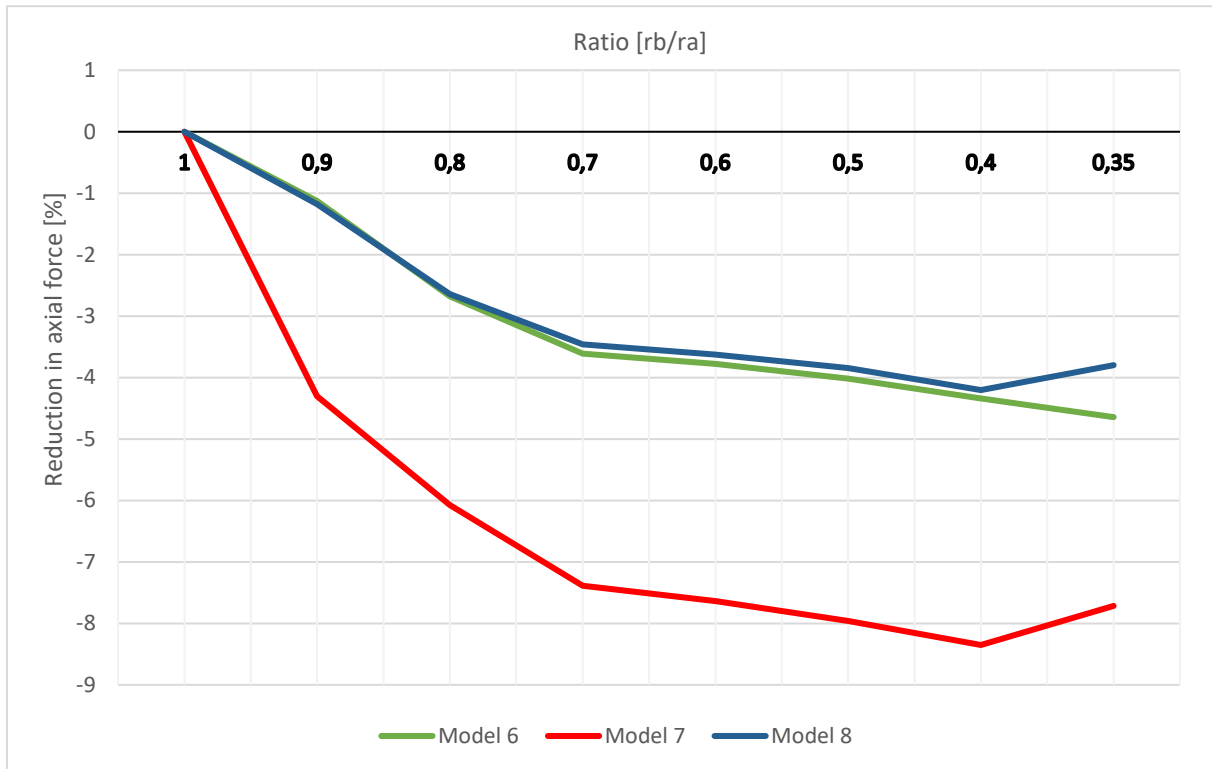


Figure 6.11: Full load.

Figure 7.12 illustrates the decrease on axial force for the elliptical arch models when half load is applied. It resembles the results for reduction of axial force in TCA for half load. All the models have the same decrease with small deviations.

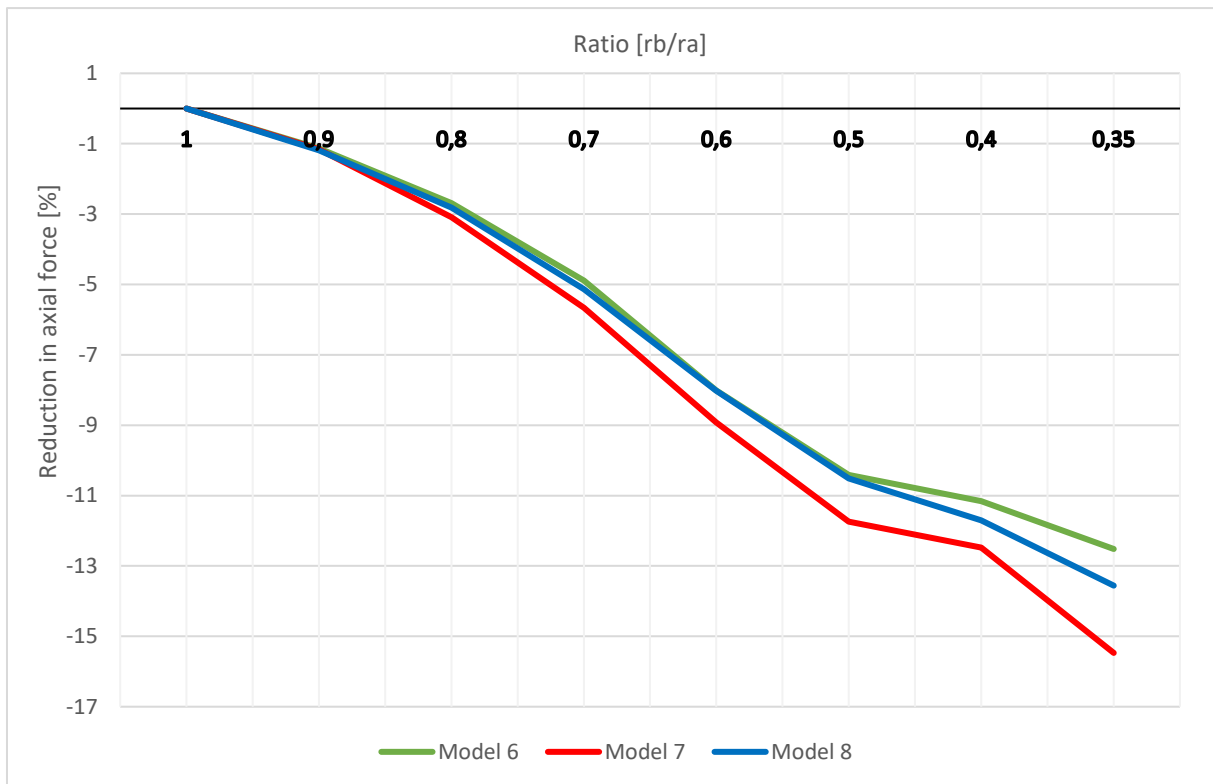


Figure 6.12: Half load.

6.5 Relaxation of hangers

Table 7.2 illustrates how many hangers that relax for the different models as the radius ratio decreases. For model 3, 4 and 5 almost no hangers relax even as the ratios get low. Over all, model 1 has the highest number of relaxed hangers for TCA. The elliptical arches show that when the ratio goes lower than 0.6 number of relaxed hangers increase, see appendix B-3.

Table 6.1: Number of relaxed hangers for det different models.

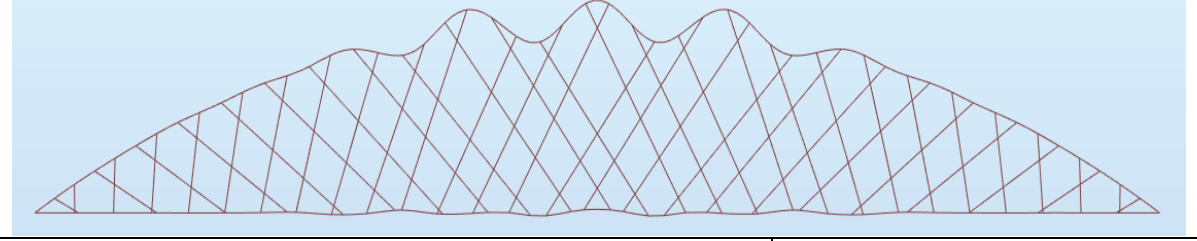
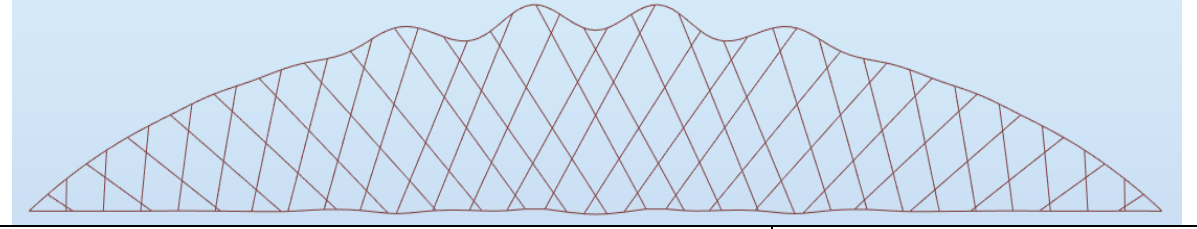
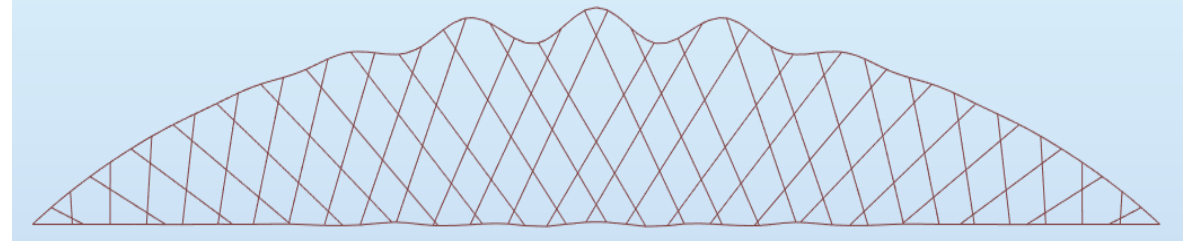
Ratio	1		0,9		0,8		0,7		0,6		0,5		0,4		0,35		0,3	
	FL	HL	FL	HL	FL	HL	FL	HL	FL	HL	FL	HL	FL	HL	FL	HL	FL	HL
Mod1	-	1	-	1	-	1	-	1	2	1	2	1	2	5	2	11	4	12
Mod2	-	1	-	1	-	1	2	1	2	1	2	1	2	4	2	7	2	12
Mod3	-	-	-	-	-	-	-	-	-	-	-	-	-	1	-	1	2	1
Mod4	-	-	-	-	-	-	-	-	-	-	-	-	-	-	-	2	2	5
Mod5	-	-	-	-	-	-	-	-	-	-	-	1	-	3	-	8	-	12
Mod6	-	1	-	1	-	1	-	1	-	3	-	8	-	12	6	20		
Mod7	-	-	-	-	-	-	-	-	-	-	-	2	8	18	-	26		
Mod8	-	-	-	-	-	-	-	-	-	3	-	7	-	14	4	24		

6.6 Comparison

6.6.1 In-plane buckling modes

Table 7.3 shows the buckling mode shapes for the different arch shapes. Buckling analysis was conducted in RSA by using full unit load on the bridges, and the stiffness of the tie was increased by changing it to a fictitious profile, IPE 800 with in-plane moment of inertia of $1,129E+08 \text{ mm}^4$.

Table 6.2: Buckling mode shape and critical coefficients for the optimal geometries [RSA].

Model A Number of wave crests: 3	Critical coef.: 2,39246e+02
	
Model B Number of wave crests: 4	Critical coef.: 2,40443e+02
	
Model C Number of wave crests: 3	Critical coef.: 2,41549e+02
	

6.6.2 Moving loads

Figure 7.13-15 show the bending moment envelopes for the moving load calculations in RSA.

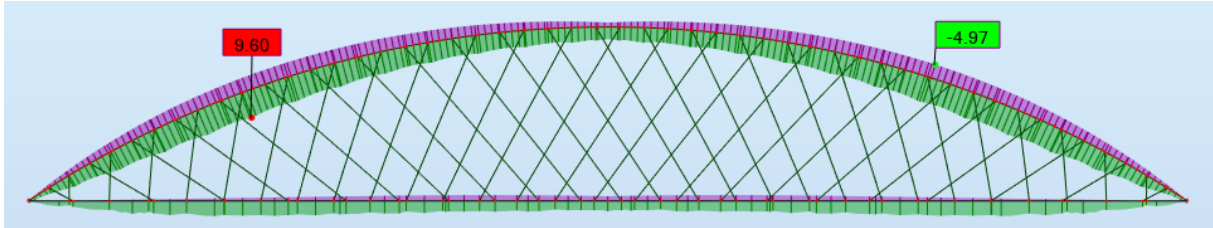


Figure 6.13: Moment envelope for model A.

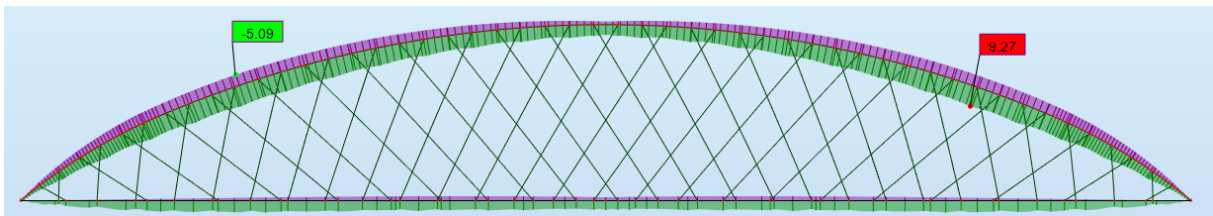


Figure 6.15: Moment envelope for model B.

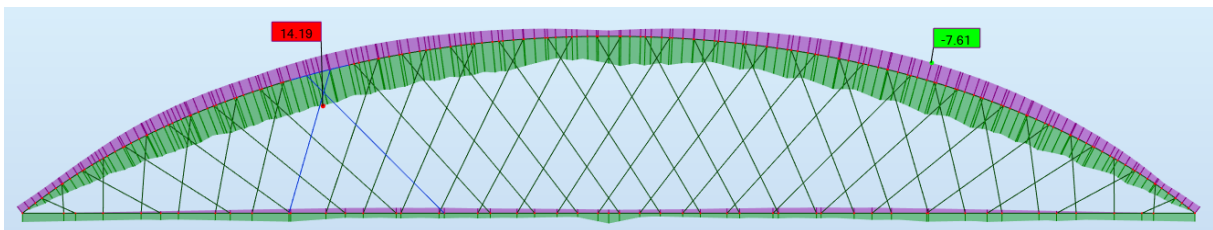


Figure 6.14: Moment envelope for model C.

6.6.3 Forces

Comparison of forces for the different shapes, see table 7.4. Values are for full unit load on the whole bridge span.

Table 6.3: Comparison of results for the different arch shapes.

Arch shape	Positive bending moment [kNm]	Negative bending moment [kNm]	Axial force (compression) [kN]	Hanger force [kN]
Model A	44,64	0,41	358,94	29,45
Model B	31,62	5,49	346,28	30,19
Model C	32,42	0,03	345,98	29,76

7 Discussion

In this chapter the results from the thesis will be discussed. The validity of the results depends on the authors accuracy of constructing all the bridge models, and the software Robot Structural Analysis.

First the different arch shapes will be reviewed by them self, before they all are compared to each other.

7.1 Circular arch

The base case of this thesis has been the circular arch shape of the network arch bridge. The circular arch shows great behavior when it comes to even distribution of axial forces in the arch, and consequently the tensile forces in the hangers are very even. This leads to small chance of relaxation of the hangers both under full and half loading of the bridge. This is the case if the optimal hanger arrangement is applied. As can be seen from table 7.2 one hanger relaxes under half load for model 1,2 and 6 which can mean that the hanger angle was a little bit off.

7.2 TCA

Deriving the formula for calculation of different radius ratios for the three-center arch shape turned out to be more time consuming than expected. In addition, the method for finding obtaining the ratios was not optimal. It required a lot of trial and error for all the models, and the ratio outputs from the calculations did not give integer numbers. So, a method of retrieving the exact ratios would be preferable.

As the positive moments decreases towards ratio 0.4-0.35 for model 1-4 (figure 7.1 and 7.2) the negative bending moments arise. When the radius ratio gets lower the shape of the arch goes towards the compression line of the arch. It is likely that it is the reason for the increase in positive bending moments. The results may indicate that the reduction of moments is very large for some of the models. For example, model 1 shows a decrease of positive moment from 44,64 kN (ratio 1.0) to 27,35 kN (ratio 0.35) when full load is applied. At the same time the negative moments increase from 0,41 kN (ratio 1.0) to 10,56 kN (ratio 0.35). So, overall it looks like the reduction of bending moments are not so large.

From the results of axial forces in figure 7.5 model 4 has the largest reduction of axial force at around 7 %. As this model has a higher rise then the others it can lead to a larger reduction of axial force. As explained in chapter 3.3.1, the shape of the arch start to resemble the behavior of a two-hinged arch when the radius ratio decreases. Therefore, it might be the reason that the reduction in arch compression force flattens out as the radius ratio decreases, this is most evident in the full load case, but there is a tendency for the axial forces to flatten out also for the half loading in figure 7.6.

In most cases the circular arch is chosen for its low production costs. For the arch itself it reasonable to believe that the production cost will not be much higher for the three-center arch. This is because the reduced curvature at the end of the arch could be limited to the first arch segment near the bridge end. The amount of welding of the arch segments would be the same. It is worth mentioning that the welding at the transition point between the curvatures must be carefully executed so that the stress will not rise at this point. Welding of hanger connections to the arch will most likely be more time consuming as the inclination of the hanger's changes as the curvature change.

7.3 Elliptical arch

A lot of the same tendencies can be seen from the calculations of the elliptical arch shaped models.

The results for the elliptical arch are taken from ratios 1.0 (circular) to 0.35. The reason for this is that a curvature with ratio lower than 0.35 gave an arch geometry where nearly no horizontal forces were transferred to the abutment. While analyzing it was also clear for all the models that there was no increase in structural behavior of the bridge when considering bending moments below ratio 0.35. On top of that the hanger arrangement had to be manually changed for radius ratios 0.4 and 0.35, as the slope of the hangers near the end became very horizontal near the bridge end.

From the constructional view the elliptical arch shape may make for an expensive arch. The manufacturing of the arch segments will most likely be more complicated as every segment must be made with unique curvature. The same goes for the hanger connections to the arch. Aesthetically the elliptical arch seems to be quite pleasing to look at. There are no transition points like for TCA which gives a more even transition.

For the elliptical arch a ratio of $\frac{r_b}{r_a} = 0.4$ has a much steeper curvature at the arch end than $\frac{r}{R} = 0.4$ for the TCA. This means that the elliptical arch has larger eccentricity (see figure 3.8) than the TCA. That may be the reason for the more sudden inclination of both positive and negative bending moments in the elliptical arch that can be seen in figures 7.7 through 7.10. It seems that no matter which model (6,7 or 8) the bending moments arise at around ratio 0.5 for the elliptical arch.

Rise of the arch

Model 4 and 7 has an increased arch rise of 34 meters. The two models have the largest decrease of axial force when full load is applied. The values are 7,24 % and 8,35 %, respectively at radius ratios 0.35. Chapter 3.3.1 implies that the axial forces will decrease with higher arch rise.

Hanger inclination

A model for hanger inclination of 40 degrees was only made for TCA. As the elliptical arch shapes gets really steep for the lowest ratios, the 40-degree inclination made modeling hard since almost all the hangers had to be manually adjusted to the tie. As this manual adjustment is a trial and error process it was decided that it should be excluded from the calculations. Model 3 has the lowest reduction in axial forces of all the TCA models when full load is applied.

Number of hangers

Number of hangers seems to mainly effect the reduction of positive bending moments for both model 5 and 8, see figure 7.1, 7.2, 7.7 and 7.8. If the hanger number is reduced, the distance between the top node of the hangers in the arch increase. This can lead to an increase of local bending moments.

Transition point

Comparing model 1 and 2 that has the same variables except for the positioning of the transition point it can be seen from figure 7.1 through 7.6 that the difference between these two models are small. This indicates that the placement of the transition point may not influence the optimal curvature that much.

7.4 Comparison

Comparing results from figure 7.1 to 7.4 gives a mean radius ratio of around 0.5 for TCA. This is based on where the reduction of positive bending moments ends for all models in figure 7.1-7.2, and where the negative bending moments start to increase for all models in figure 7.3-7.4.

Comparing results from figure 7.7 to 7.10 gives a mean radius ratio of around 0.6 for the elliptical arch. This is based on where the reduction of positive bending moments ends for all models in figure 7.7-7.8, and where the negative bending moments start to increase for all models in figure 7.9-7.10.

This is quite similar to what Teich found out in his research, see chapter 3.3.1.

The in-plane buckling results from table 7.3 shows that there is slightly higher in-plane buckling resistance for model B and C compared to model A. The buckling resistance is dependent on the compressive forces in the investigated element. Since model A has a compressive axial force in the arch of 358,94 kN and model B and C has 346,94 kN and 345,98 kN, respectively, it could be the reason for the slightly larger buckling resistance.

The bending moment envelopes for the moving load gives very similar results for model A and B. Bending moments for model C is higher. Model 6 (same geometry as model C) in table 7.1 shows that 3 hangers relax under half loading. If one hanger relaxes the bending moment arises as the distance between the top nodes of the hanger's doubles. If Model C is more likely to have relaxed hangers than the other two models, this might be the reason for the much larger bending moments.

When comparing the forces for the different models A, B and C the results show that model B and C has a reduced positive bending moment of 29,2 % and 27,4 %, respectively. The negative moment increases slightly for model B compared to model A. For the axial forces the reduction of 3,5 % for model B and 3,6 % for model C.

8 Conclusion

The research question that I am going to answer in this thesis is: *How can the optimal curvature of a network arch bridge be obtained?* Two sub-questions were formed to help answering the research question:

How will different curvatures effect the moments at the arch end?

Two model types are analyzed in this project to see if they can improve in the circular arch shape. The three-center arch (TCA) and the elliptical arch. The models are constructed by incrementally decreasing the radius ratio at the bridge. Results are obtained by applying simple loads on the models. The results show that when applying simple loads on the whole bridge span and half bridge span, the bending moments decrease towards an optimal radius ratio. When designing bridges with elliptical arches or three-center arches it is advisable to use reduced radius ratios, the results indicate a radius ratio that should not be lower than 0.6 and 0.5, respectively. Investigation of these radius ratios in 3D-model with full design load is needed for these values to be validated.

What kind of arch shape will improve the structural behavior most?

From the analysis done in this thesis I cannot conclude with whether the three-center arch or the elliptical arch improves the structural behavior most. What I can conclude with is that both elliptical arch and TCA give better resistance of the bending moments at the end of the arch then by using circular arches.

9 Suggestions for further work

For further work a cost-benefit analysis would be interesting to investigate. As the design of the arch often is dependent on cost rather than structural behavior it would be interesting to see if production of for example a three-center arch is more expensive than a circular arch.

An LCA analysis could identify what changes in environmental impact in could mean to change to a more optimal arch shape.

Also, a comparison between a circular arch and an arch with reduced radius where they both are tested for all design verifications.

10 References

- [1] Bridges of Dublin. (2019). *Arch* [Online]. Available: <http://www.bridgesofdublin.ie/bridge-building/types/arch>
- [2] A. Sinopoli, *Arch Bridges*. Rotterdam: A.A. Balkema, 1998.
- [3] B. Bradly. (02.05.2019). [Online]. Available: <http://www.builderbill-diy-help.com/three-centre-arch.html>
- [4] M. Yashinsky. (2009, 03.05.2019). *Shanghai's Bridges: Zhejiang Road Bridge* [Online]. Available: <http://www.bridgeofweek.com/2009/08/shanghai-bridges-zhejiang-road-bridge.html>
- [5] A. Pipinato, *Innovative Bridge Design Handbook 1.*, ed.: Butterworth-Heinemann 2015. [Online]. Available: <https://www.elsevier.com/books/innovative-bridge-design-handbook/pipinato/978-0-12-800058-8>.
- [6] P. Tveit, "Systematic Thesis on Network Arches," p. 83 Available: https://home.uia.no/pert/index.php/Systematic_Thesis
- [7] S. M. Johannesen, "Dimensjonering og byggemetode av nettverksbru," Master, NMBU, Ås, 2014.
- [8] P. Tveit, "The Network Arch," Teknisk rapport 01.07.16, 2016, Available: https://home.uia.no/pert/index.php/The_Network_Arch.
- [9] Strilen. (2015). *Stengt for vedlikehold* [Online]. Available: Stengt for vedlikehold
- [10] *Tsukani Bridge* [Online]. Available: http://www.civil.eng.osaka-u.ac.jp/str/rec/tsukani/tsukani_eng.html
- [11] I. Albina Co. *Bending profiles: beams/wide flange* [Online]. Available: <https://www.albinaco.com/bending-profiles/beams>
- [12] J.-P. Lebet and M. A. Hirt, *Steel Bridges*, 1. ed. Switzerland: Taylor & Francis Group Ltd, 2013.
- [13] S. Teich, "Beitrag zur Optimierung von Netzwerkbogenbrücken," Dr.-Ing., Faculty of Civil Engineering, University of Dresden, Dresden, 2012.
- [14] A. Pipinato, "Structural analysis and design of a multispan network arch bridge," PhD, 2016.
- [15] B. Bruun and F. Schanack, "Calculation of a double track railway network arch bridge applying the European standards," Master, Technische Universität Dresden, Høgskolen i Agder, Grimstad, 2003.
- [16] T. J. M. Smit, "Design and construction of a railway arch bridge with a network hanger arrangement," M.Sc, Iv-Infra, Delft University of Technology, Delft, 2013.
- [17] Robot Structural Analysis. (2015). *Non-linear Static Analysis* [Online]. Available: <https://knowledge.autodesk.com/support/robot-structural-analysis-products/learn-explore/caas/CloudHelp/cloudhelp/2015/ENU/Robot/files/GUID-FB3C86D3-0E30-43A6-82D6-6C50F429FA0D-htm.html>
- [18] F. Schanack, "In-plane arch buckling of network arch bridges," presented at the World Steel Bridge Symposium, San Antonio, TX, 2009. Available: https://www.researchgate.net/publication/301198220_In-Plane_Arch_Buckling_of_Network_Arch_Bridges
- [19] M. Yang and S. Gajan, "Strength-based differential tolerable settlement limits of bridges," p. 14. doi: 10.1177/1369433217706779

11 Table of appendix

Appendix A: Values for radius ratios.

Appendix B:

- B-1: Bending moments
- B-2: Axial forces
- B-3: Hanger forces and relaxation of hangers

Appendix C: A3-poster.

Appendix D: Administrative documents (Progress plan and minutes of meeting).

Appendix E: Deduction of radius geometry for TCA.